Hydrogen Storage in Molecular Clathrates

Viktor V. Struzhkin,*,† Burkhard Militzer,† Wendy L. Mao,‡ Ho-kwang Mao,† and Russell J. Hemley†

Carnegie Institution of Washington, Geophysical Laboratory, 5251 Broad Branch Road, NW, Washington, DC 20015, and Lujan Neutron Scattering Center, Los Alamos National Laboratory, Los Alamos, New Mexico 87545

Received December 7, 2006

Contents

1. Introduction

The technology of using hydrogen as an environmentally clean and efficient fuel is an active research area worldwide.[1,2] One of the major challenges in establishing a hydrogen-based economy is effective storage and delivery of hydrogen. Liquid hydrogen, which has modest densities of 70 g/L, is currently the most commonly used form in prototype automobiles, and is very energy intensive—up to 40% of the energy content must be spent to liquefy hydrogen at its very low condensation temperature (20 K). This low temperature cannot be provided by practical and inexpensive cooling agents, e.g., liquid nitrogen (>77 K); hence, the continuous boil-off of liquid hydrogen poses problems to on-board storage. Compressed hydrogen gas, the second most commonly used storage system, typically only holds 15 g/L at 35 MPa. Higher pressures could hold higher hydrogen densities, but this is complicated by safety and logistical concerns. Other storage methods, including molecular hydrogen adsorption on solids with a large surface area (e.g., metal−organic frameworks or carbon nanotubes) and bonded atomic hydrogen in hydrocarbons or in metal hydrides, have been developed extensively to address key issues of hydrogen content, $P-T$ conditions of synthesis and storage, and on-board hydrogen release.[2] Hydrogen clathrates have been discovered and suggested as a candidate material for hydrogen storage very recently.[3−5]

Storage of hydrogen in supermolecular compounds consisting of simple molecules represents an alternate approach. One of the first studied supramolecular systems was the cagelike host−guest clathrate structure. In clathrates, "two or more components are associated without ordinary chemical union, but through complete enclosure of one set of molecules in a suitable structure formed by another".[6] The major subject of this review is clathrate-based compounds of hydrogen from the point of view of both experiment and theory. These clathrate materials have potentially important future energy applications including hydrogen-fueled cars, energy storage, and distribution grids.

Clathrate materials have evolved from scientific curiosity to an active research field since their discovery in 1810. Davy[7] discovered that a solid is formed when an aqueous solution of chlorine (then known as oxymuriatic acid) was cooled below 9.0 °C, and Faraday suggested that the composition of the new solid was nearly 1 part of chlorine and 10 parts of water.[8] It is now known that there are many species which can combine with water and form nonstoichiometric solid compounds. Typical examples of hydrate-forming substances include CH_4, CO_2, and H_2S. The terms "gas hydrate" and "clathrate hydrates" have been used for these solids.[9]

Clathrate research had purely academic interest until 1934. At that time, the oil and gas industry in the United States was growing rapidly, and the plugging of natural gas pipelines due to formation of clathrate hydrates of natural gas became a significant problem.[10] Research efforts on natural gas hydrates were initiated by industry, government,

* Corresponding author. Telephone: 202-478-8952. Fax: 202-478-8901. E-mail: v.struzhkin@gl.ciw.edu.
† Carnegie Institution of Washington, Geophysical Laboratory.
‡ Los Alamos National Laboratory.

10.1021/cr050183d CCC: $65.00
Published on Web 09/13/2007

Viktor V. Struzhkin holds a B.S. and M.S. in physics from Moscow Institute of Physics and Technology (1980) and a Ph.D. in solid-state physics from Institute for High-Pressure Physics, Russian Academy of Sciences (IHPP, RAS) (1991). He is a staff member of the Geophysical Laboratory. At the Carnegie Institution, he pioneered a suite of transport measurements in diamond anvil cells, succeeding in measurements of superconductivity at very high pressures in excess of 200 GPa (2 million atm). He is a recognized expert in a multitude of experimental techniques in diamond anvil cells, including transport measurements and optical and synchrotron spectroscopy. His research interests cover condensed-matter physics, simple molecular solids, the chemistry and physics of the Earth's mantle and core, and high-pressure materials science.

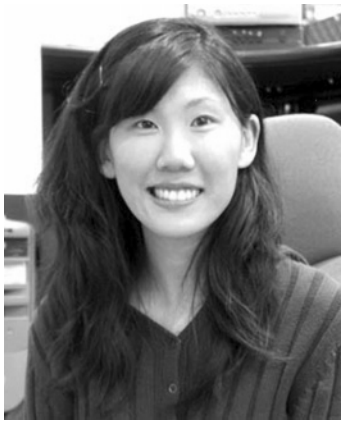

Wendy Mao received her B.S. in 1998 from the Department of Materials Science and Engineering, Massachusetts Institute of Technology, and Ph.D. in 2005 from the Department of the Geophysical Sciences, University of Chicago, under the supervision of Dion Heinz. She is currently a J. R. Oppenheimer Fellow at Los Alamos National Laboratory, working under the supervision of Yusheng Zhao and Donald Hickmott, investigating hydrogen storage in molecular compounds. Starting in August 2007, she will be an Assistant Professor at Stanford University with a joint appointment in the Department of Geological and Environmental Sciences and the Photon Science Department of the Stanford Linear Accelerator Center. Her research interests focus on understanding the behavior of materials at high pressure.

Burkhard Militzer received his diploma in physics at the Humboldt University in Berlin, Germany, under the supervision of Werner Ebeling, and he obtained his Ph.D. from the University of Illinois at Urbana–Champaign in 2000 under the supervision of David Ceperley. After working for 3 years as a postdoc at the Lawrence Livermore National Laboratory, he joined the Geophysical Laboratory of the Carnegie Institution of Washington as Staff Associate in 2003. His research is focused in first-principles computer simulation of materials at high pressure and the applications to planetary interiors.

Ho-kwang (David) Mao received his B.S. in Geology (1963) from the National Taiwan University and his M.S. (1966) and Ph.D. (1968) from the University of Rochester, where he conducted high-pressure deep Earth research under the guidance of Professors Bill Bassett and Taro Takahashi. He started as a Postdoctoral Fellow working with Dr. Peter M. Bell at the Geophysical Laboratory, Carnegie Institution of Washington, and later became a Staff Geophysicist there, a position he holds to this day. During the past four decades, he has pioneered the development of high-pressure diamond anvil cell techniques and a wide range of synchrotron X-ray, neutron, optical, electrical, and magnetic probes for *in-situ* diagnosis of samples under extreme pressures and temperatures. His research interests cover high-pressure condensed-matter physics, high-pressure chemistry, high-pressure crystallography, chemistry of the Earth's mantle and core, deep Earth geophysics, physics and chemistry of giant planetary interiors, and high-pressure materials science.

and academia[11] to understand these materials. The crystal structure of gas hydrates was discovered by X-ray diffraction studies in the 1950s. The term "clathrate" was coined in 1948 by Powell, who discovered inclusion compounds of hydroquinone.[6] He found that guest atoms are held hostage in cages of a host ("clathratus"—Latin for "enclosed or protected by cross bars of a grating") and the distances between the guest and host atoms are of the order of typical van der Waals distances (no conventional chemical bonds between the guest and the host). This discovery aided the development of a statistical thermodynamic model for the hydrate as a solid solution.[12]

From the experimental perspective, pressure can serve as a unique tool to synthesize novel crystalline compounds in which molecular hydrogen and other simple molecules can be stored. Such materials have only been discovered very recently; reconnaissance studies have been conducted on a small number of simple molecular systems such as H_2-CH_4,[5,13] H_2-H_2O,[4,5,14] and H_2-Ar.[15] Each system already represents a growing research area with technological potential. These compounds can retain an enormous amount of hydrogen: $Ar(H_2)_2$ has 9.2 mass % molecular hydrogen, $H_2(H_2O)_2$ holds 5.0 mass % molecular H_2 (a total of 15.6 mass % if all H atoms are counted), and $(H_2)_4(CH_4)$ holds 33.4 mass % molecular hydrogen (total of 50 mass % H),

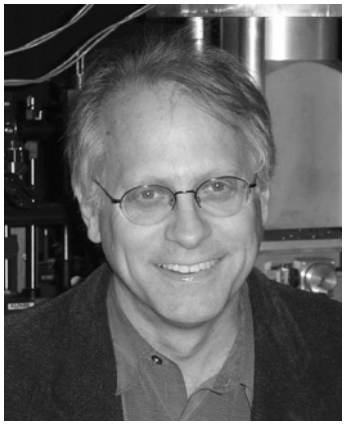

Russell J. Hemley grew up in California, Colorado, and Utah, and attended Wesleyan University, where he studied chemistry and philosophy (B.A., 1977). He did his graduate work in physical chemistry at Harvard University (M.A., 1980; Ph.D., 1983). After a postdoctoral fellowship in theoretical chemistry at Harvard (1983–84), he joined the Geophysical Laboratory as a Carnegie Fellow (1984–86) and Research Associate (1986–87), and he became a Staff Scientist in 1987. He has been a visiting Professor at the Johns Hopkins University (1991–92) and at the Ecole Normale Superieure, Lyon (1996). He is the recipient of the 1990 Mineralogical Society of America Award, and he is a Fellow of the American Physical Society, the American Geophysical Union, and the American Academy of Arts and Sciences. He was elected as a member of the National Academy of Sciences in 2001 and became a member of JASONS in 2003. In 2005, he was awarded the Balzan Prize in Mineral Physics. He has been an author on over 440 publications.

all significantly above DOE targets[16] (see section 2.1.2 for a detailed comparison). Hydrogen is retained by weak van der Waals forces and interactions in these solids, and can be readily released by increasing temperature (*T*) or decreasing pressure (*P*). These hydrogen storage compounds are formed at high *P* and low *T*, and hydrogen is released automatically near ambient *P* and *T*.

By varying *T* and chemical composition (denoted by an arbitrary constituent X), the relatively high synthesis pressure—which has been the main obstacle for the molecular compounds to be a viable hydrogen storage material so far—can be reduced. Areas of research include exploring the $P-T-X$ space for each of the following three categories of hydrogen materials: (*i) molecular hydrogen storage (MHS) in hydrocarbons, (ii) MHS in clathrates, as well as (iii) MHS in other inert components.* An important goal has been to acquire fundamental understanding of the different classes of materials. In order to search for, and to optimize, a practical hydrogen storage material, only a few simple systems (H_2-CH_4, H_2-H_2O, and H_2-Ar) have been studied so far, and in each system, unexpected compounds have been discovered. A larger number of other binary and multicomponent systems may have the potential to be developed into fuel systems. This review focuses on hydrogen clathrate hydrates as well as molecular (i.e., van der Waals) compounds that may be highly promising systems for MHS.

High-$P-T$ techniques provide an important means to synthesize novel MHS materials, including materials that can be quenched to ambient or near ambient conditions. Theoretical calculations complement the effort by providing guidance on possible structures. Specifically, the clathrates can be modeled in the calculations, and their stability, structure, and bonding can be examined to identify the most stable materials suitable for practical applications.

2. Hydrogen in Clathrate Hydrates

2.1. Binary Hydrogen Hydrates

2.1.1. Discovery

Dyadin et al.[3] studied the H_2O-H_2 system by differential thermal analysis and found a temperature region exhibiting anomalous melting behavior and kinetics of ice melting at hydrogen pressures of 100−360 MPa. They hypothesized that a clathrate phase of hydrogen hydrate was formed in this pressure range. Following that work, the clathrate phase *sII* of hydrogen hydrate was synthesized by Mao et al.[4] from a liquid at a pressure of about 200 MPa and at −24 °C. Mao et al. suggested that four hydrogen molecules are stored in a large *sII* clathrate cage, and two hydrogen molecules are stored in a smaller cage. Lokshin et al.[17] studied the composition of this phase by neutron diffraction and found that $D_2/D_2O = (32 + x)/136$, where *x* varied from 0 to 16 depending on *P* and *T* (see Table 1). The value of $x = 16$ (one hydrogen molecule in small cages of *sII* clathrate) corresponds to the 3.9 mass % hydrogen content in the clathrate. Because the pressures of >200 MPa are expected within ice planet satellites, a study of the H_2O-H system at these conditions is of considerable interest in planetary science.[4] The implications of the newly discovered clathrate as a hydrogen storage material were further explored in refs 5 and 18. These earlier studies were followed by other investigations by the broader community. The subsequent work elaborated on the original findings as described in the following sections.

2.1.2. Clathrate Structures and Storage Potential

Many structural frameworks with slightly different energies can be formed from water molecules due to their tetrahedral coordination and hydrogen bonding topology determined by the "ice rules"[19,20] and by the ordering of the hydrogen bonds. The structures of the gas hydrates may be represented as a set of close-packed polyhedra (Figure 2) built from the water molecules, with neighboring polyhedra having common faces. The most common gas hydrate structures, cubic *sI* and *sII*, contain two types of different sized cages (Figures 3 and 4). The least deformed water molecules' polyhedron is a pentagonal dodecahedron (*D*-cavity or small cavity), which occurs in most clathrate

Table 1. Idealized *sI*, *sII*, and *sH* Clathrate Hydrate Structures

structure	unit cell formula	unit parameters (in Å)	limit of hydrate number (all cavities occupied/large cavities occupied)	examples of hydrates
sI (cubic structure I)	$6T\cdot 2D\cdot 46H_2O$	12.0	5.75/7.66	$H_2S\cdot 6H_2O$ $CH_4\cdot 6H_2O$
sII (cubic structure II)	$8H\cdot 16D\cdot 136H_2O$	17.1	5.66/17	$Ar\cdot 6H_2O$ $SF_6\cdot 17H_2O$
sH (hexagonal structure *H*)	$3D\cdot 2D'\cdot 1I\cdot 34H_2O$	$a = 12.26$ $c = 10.17$	5.66/34	see ref 25

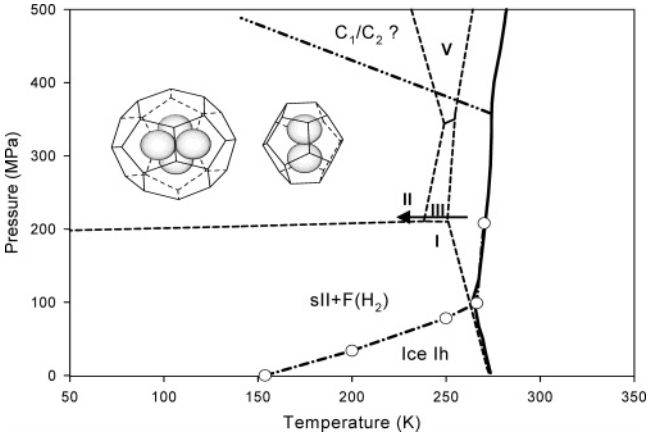

Figure 1. Phase diagram of the hydrogen−water system in relation to the hydrogen clathrate hydrate. The solid line is from ref 3. The open circles and dash-dotted lines are from ref 44. Dashed lines show the boundaries between different phases of ice. The actual filling of the *sII* clathrate cages by H_2 molecules over the stability range has not been established yet. The composition of hydrogen clathrate hydrate at the ice *Ih*−*sII* boundary is compatible with just one hydrogen molecule in both large and small cages.[128] The arrow shows the path used by Mao et al.[4] for synthesis of the *sII* clathrate hydrate.

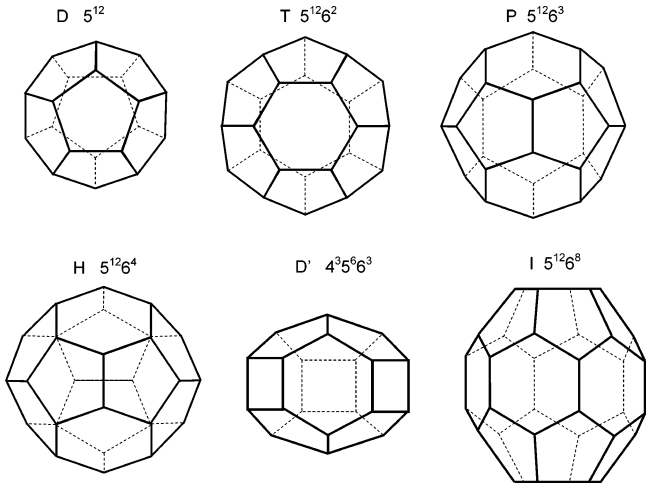

Figure 2. The major building blocks of the clathrate lattice—Allen's polyhedra.[62] *D*, pentagonal dodecahedron (12 pentagonal faces); *T*, tetrakaidecahedron (12 pentagonal and 2 hexagonal faces); *P*, pentakaidecahedron (12 pentagonal and 3 hexagonal faces); *H*, hexakaidecahedron (12 pentagonal and 4 hexagonal faces); *D*′, irregular dodecahedron (3 square, 6 pentagonal, and 3 hexagonal faces); *I*, icosahedron (12 pentagonal and 8 hexagonal faces).

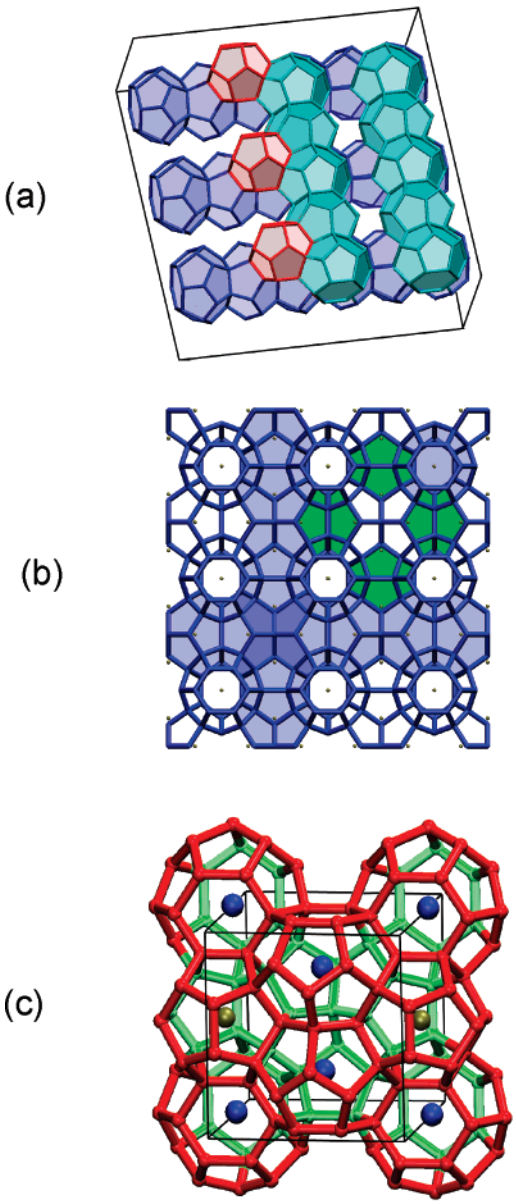

Figure 3. (a) Clathrate *sI* structure consisting of linear chains of large *T* cages that share hexagons. Two sets of chains are shown in blue and turquoise. The third set of chains running vertically was omitted for simplicity. Small *D* cages shown in red fill the remaining voids. (b) Layer of the clathrate *sI* structure. Two examples for linear chains of large *T* cages are shown in blue. A selection of small *D* cages is colored green. The small dots mark the cage centers of the large *T* cages. (c) Cubic unit cell of the clathrate *sI* structure[129] with a selected number of cages. Blue spheres mark the centers of the large *T* cages, and brown spheres are at the centers of the small *D* cages.

hydrate structures. It is the only hydrate cage that has planar faces with both equal edges and O−O−O angles. In the *D* (5^{12}) cage there is only a 1.5° departure of the O−O−O angles from the tetrahedral angles of ice *Ih* and only 3.5° departure from the free water angle; the O−O bond lengths exceed those in ice by 1%. However, the pentagonal dodecahedron does not fill the available space and requires the presence of cages of larger sizes (*T*, *P*, *H*, *D*′, *I*—large cavities). Depending on their size, the guest molecules can be accommodated only in the large cages or in both types of cages. It is not necessary to have 100% occupation of the large cages for the formation of the clathrate hydrate,[21] but it is quite common for the large cages to be filled to nearly 100% occupancy;[22] occupation of the small cages may vary from 0 to 100%.[22] The clathrate structures have been examined in detail by von Stackelberg and Müller.[23] They divided the structures into two types, type *sI* (or "structure I") and type *sII*: type *sI* contains small cages in a 1.20 nm size unit cell in space group *Pm*3*n*, and type *sII* contains larger cages in a 1.73 nm size unit cell in space group *Fd*3*m*.[9,24] The most commonly found among these is the *sII*, in which there are 17 H_2O molecules per guest molecule;[23] its ideal unit cell contains 136 H_2O molecules forming 16 small (*D*) and 8 large (*H*) cages[9,24] (Figure 4). Clathrate hydrates have been found to form crystals of hexagonal symmetry (space group *P*6*mmm*).[25] These are called "type *H*" or structure *H* clathrates (*sH*) (Figure 5).

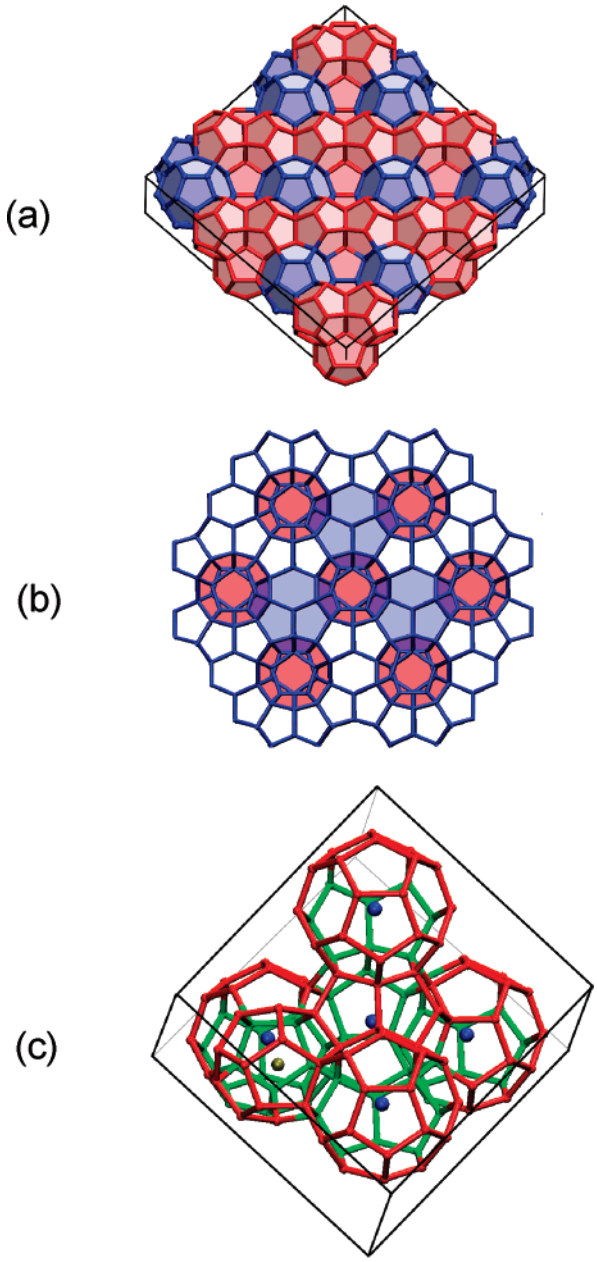

Figure 4. (a) Clathrate *sII* structure consisting of small *D* cages shown in red and large *H* cages shown in blue. The small cages are shared by pentagons and form linear chains along the [110] direction that are displayed horizontally. (b) Layer of the clathrate *sII* structure with small cages shown in red and large cages shown in blue. (c) Cubic unit cell of the clathrate *sII* structure[130] with a selected number of cages. The centers of the large cages (blue spheres) form a diamond lattice. As illustrated for the middle cage, each large cage shares a hexagon with four neighboring large cages. The remaining voids are filled with small cages (e.g. the cage with the brown sphere at its center).

Clathrate hydrates with a single guest component at moderate pressures (up to tens of MPa) have been the most extensively studied.[26,27] The structures of the clathrate hydrates formed in these systems in most cases were determined by diffraction methods at atmospheric pressure and low temperature. It was found that small molecules such as nitrogen and oxygen form *sII* hydrates, whereas, earlier, these gases were regarded as typical *sI* formers.[28,29] Table 1 lists the structural units and the number of water molecules in *sI* and *sII* structures. For *sII* clathrate hydrates having 8 large and 16 small cages, the content (by mass) of hydrogen

Table 2. Comparison of Hydrogen Storage Characteristics for H_2-H_2O and H_2-CH_4 Materials

		H_2 mass %	kWh/kg	kWh/L	kg/L
sII	$H_2(H_2O)_2$	5.265	1.8	1.5	0.83
C_2	$H_2(H_2O)$	11.2	3.7	3.5	0.95
HM4	$(H_2)_4(CH_4)$	33.4	11.1	~10	~0.9
DOE target	2005	4.5	1.5	1.2	0.8
DOE target	2010	6	2	1.5	0.75
DOE target	2015	9	3	2.7	0.90

calculated as $H_2/H_2O = (8 \times 4 + 16 \times 1)/136$ (4 H_2 molecules in the large *H* cage and 1 molecule in the small *D* cage) is 3.9%.

The hydrogen−water system has already yielded two potential hydrogen storage materials, a hydrogen clathrate hydrate with classic *sII* structure[4] and a filled ice phase C_2[14]. The phase *sII* was synthesized at 250−600 MPa and 249 K; it contains 50 g/L hydrogen (5.3 mass %) and was successfully recovered to ambient *P* (0.1 MPa) at 77 K, thus demonstrating the potential for hydrogen storage.[4] Neutron scattering studies of deuterated water and deuterium at 220 MPa and 200−270 K showed that smaller cages hold just one deuterium molecule.[17] The kinetics of the reactions or isotope effects may contribute to the different results reported.

A practical hydrogen storage method must satisfy a number of requirements: (1) high hydrogen content per unit mass, (2) high hydrogen content per unit volume, (3) moderate synthesis *P* (preferably <400 MPa, the pressure that can be reached by a simple compressor), (4) near ambient *P* and moderate *T* for storage, (5) easy hydrogen release, and (6) environmentally friendly byproducts, if any. Storage of hydrogen in molecular compounds provides an attractive alternative to other approaches.[16] Table 2 lists some compounds of this type holding quantities of hydrogen that exceed DOE targets[16] of 2005−2015 in both kWh/kg (energy delivery capacity) and kWh/L. The H_2O host molecules would be an environmentally very friendly byproduct, while the CH_4 host molecules could be used as a supplemental fuel (albeit not environmentally friendly) or just retained as a storage medium. The challenge is that these materials currently require too high a pressure (several hundreds of MPa) for synthesis and retention to be practical.

At sufficiently low temperature, hydrogen is retained in the solid by weak bonding to host molecules under moderate synthesis pressure (P_s) and temperature (T_s). The solid is cooled down to moderately low temperature (T_q), and the pressure is released to (P_q), and the hydrogen-containing solid is recovered at ambient pressure (quenched). The stored hydrogen can be released by warming up toward a temperature (T_a) for final applications. This low-temperature synthesis route has been demonstrated for $H_2(H_2O)_2$,[5] which is quenchable to ambient *P* at moderately low *T* (77 K). The $H_2(H_2O)$ "filled ice" and $(H_2)_4(CH_4)$ "molecular ice" compounds contain higher amounts of hydrogen and can be quenched to moderate *P* at low *T* (500 MPa, 77 K and 200 MPa, 77 K, respectively[5]). Ideally, the bonding to the ice host helps to stabilize molecular hydrogen in the crystalline compounds at moderately low *P*−*T*, yet is sufficiently weak for easy hydrogen release. Other gas−ice systems are known to contain a great number of stable and metastable phases,[30−33] and new phases of ice are still being discovered.[34−38] By analogy, new compounds are expected in the hydrogen−ice system by exploration of the multicomponent (e.g., $H_2O-CH_4-H_2$) system along different *P*−*T* paths. The very large

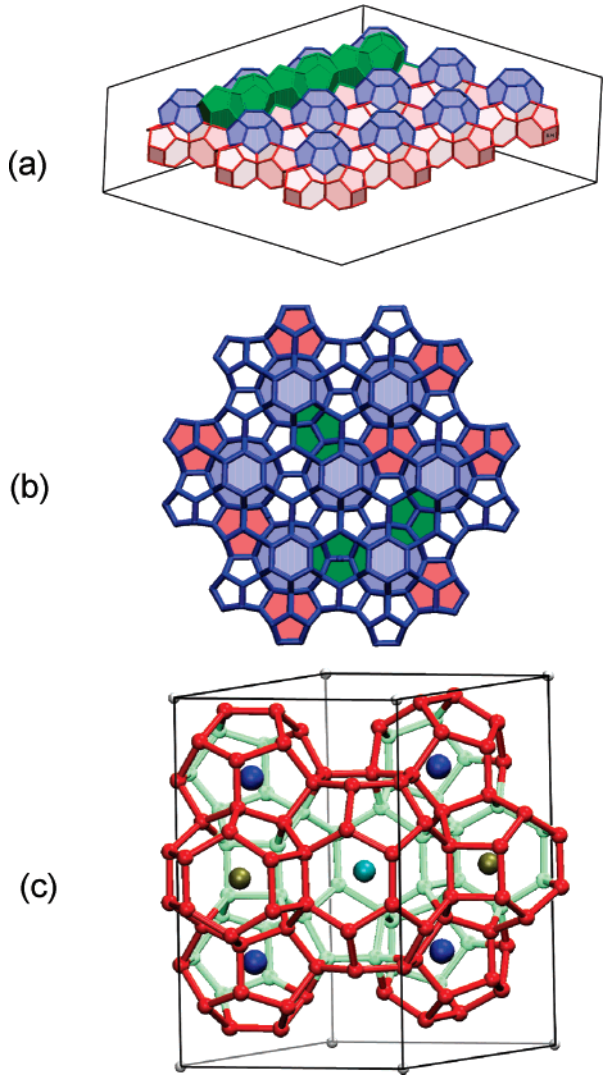

Figure 5. (a) One layer of the clathrate *sH* compound is shown. The large barrel *I* cages shown in blue are arranged on a hexagonal lattice. Each barrel shares hexagons with barrel cages in the neighboring layers. Within the displayed layer, each barrel cage shares hexagons with six D' cages that are shown in red. These cages share squares between them. The remaining voids are filled with linear chains of small *D* cages that are displayed in green. (b) A layer of the clathrate *sH* structure. The barrel cages (blue) are arranged on a hexagonal lattice. The selected set of *D* and D' are shown in red and green, respectively. (c) Hexagonal unit cell of the clathrate H structure[131] with a selected number of cages. The turquoise, brown, and blue spheres are located at the centers of the *I*, D', and *D* cages, respectively (see Figure 2 for the notation of the cages).

hysteresis and the path-dependent phase relationships documented at low *T* open opportunities for metastable growth and stabilization of hydrogen-rich phases. Future avenues for exploration may include investigation of larger guest molecules to stabilize the H_2O framework structure of other clathrate structures (*sI*, *sH*), and filled ices, and studies of the possibility of multiple occupation of H_2 in cages of other structures.

With the accelerating advances in static compression techniques in recent years, an increasing number of new materials have been synthesized both under *P* and recovered to ambient *P*.[39] Arguably, the most important material created under pressure and recovered for manifold uses is diamond, which forms the basis of a multibillion dollar a year industry. Recent developments suggest great potential for finding or exploiting other high-pressure materials. Low temperature hinders transition reversal and preserves high-pressure phases to near ambient pressure, as was demonstrated for the nonmolecular phase of nitrogen brought to low pressure from 200 GPa.[40] The ongoing research of the hydrogen storage in clathrates explores the moderately low (77−300 K) to moderately high (300−450 K) temperature range to search for new compounds capable of retaining a significant amount of hydrogen. However, the compounds that are formed at relatively high $P-T$ conditions may be decompressed at moderately low *T*. Similar strategies may help in the search for novel carbon clathrate materials for hydrogen storage, albeit at higher $P-T$ synthesis conditions and with the use of various starting carbon-containing materials (e.g., graphite, hydrocarbons, etc.).

2.1.3. Clathrate Formation

In the original work of Mao et al.,[4] hydrogen hydrate-*sII* was studied in the $P-T$ range of 0.1−600 MPa and 77−300 K in diamond anvil cells (Figures 6 and 7). Samples initially at 250−600 MPa and 300 K separated into two phases, A and B. Liquid water in region A and fluid hydrogen in region B have little mutual solubility, as indicated by the absence of the O−H Raman vibration in the hydrogen region and very weak hydrogen molecular rotons and vibrons in the water region.[41,42] During isobaric cooling, the sample changed suddenly at 249 K. Reaction rims grew between regions A and B while the main body of region A first darkened, due to the infiltration of hydrogen and nucleation of a new phase, and then cleared up after the new phase completely took over that region. The volume of region A increases by 40 (±2) % as the result of incorporation of hydrogen into H_2O to form a hydrogen clathrate. As the water solidified into the clathrate, the fluorescence peaks of ruby grains trapped in the clathrate broadened due to nonhydrostatic stress. The hydrostaticity and overall appearance of region B, on the other hand, remained unchanged while its size decreased due to the incorporation of hydrogen into the growing hydrogen clathrate. The formation and decomposition of the new clathrate show a large hysteresis. Similar to various phases of ices,[30,43] the clathrate can be quenched to ambient *P* at low *T*. At 300 MPa, the clathrate was first observed at 249 K on cooling, while, on subsequent warming at this pressure, the clathrate remained until reaching 280 K, above which it began gradually decomposing into water and hydrogen. When the sample was isothermally decompressed from 300 to 0.1 MPa (ambient pressure) at 77 K, hydrogen in region B vanished, indicating the complete reduction in the pressure and the escape of any unattached hydrogen gas. Meanwhile, hydrogen vibrons and rotons in region A remained unchanged, indicating the successful storage of bonded hydrogen in the clathrate. The main low-frequency vibron persisted upon warming at a rate of 0.2 K/min at ambient pressure while the weak vibrons at higher frequency than $Q_1(1)$ of pure hydrogen gradually disappeared. Eventually, the clathrate disintegrated and released hydrogen at 140 K. The described technique deals with very small sample volumes, and the kinetics of the transition should not be of critical importance, as is the case in larger volume devices. The reader interested in the details of clathrate phase equilibria studies in larger volumes should refer to the review book by Sloan.[27]

Different synthesis routes may significantly affect the kinetics of clathrate formation. Lokshin and Zhao[44] have

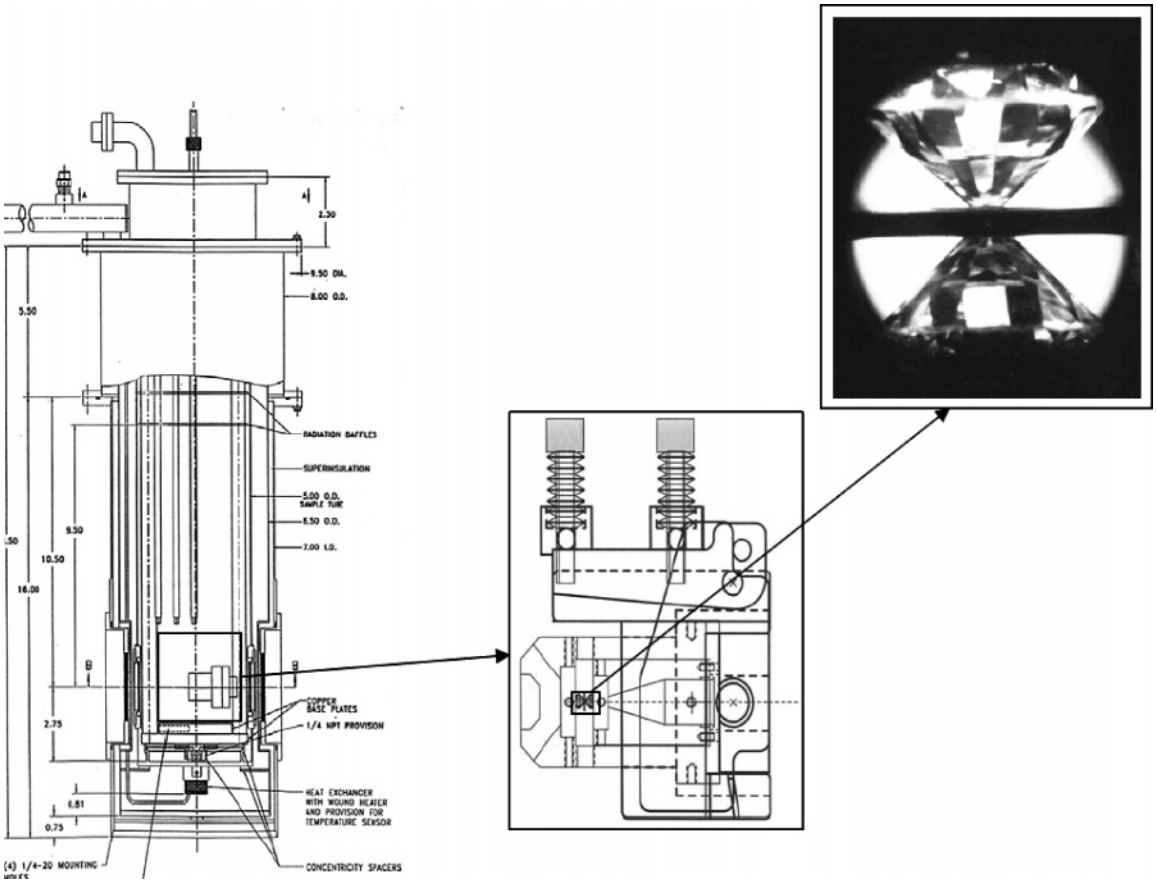

Figure 6. Experimental setup for hydrogen clathrate synthesis and measurements. The pair of diamond anvils is holding the sample enclosed in a metallic gasket; the anvils are mounted inside the diamond anvil cell with the lever arm assembly for pressure generation. The cell in the lever arm is placed inside of a cryostat (4−300 K) having optical access through sapphire windows. The pressure in the cell can be changed *in situ* at low temperature and monitored by ruby fluorescence.[132] Parts of the figure are reprinted with permission from ref 68. Copyright 2004 Elsevier B. V.

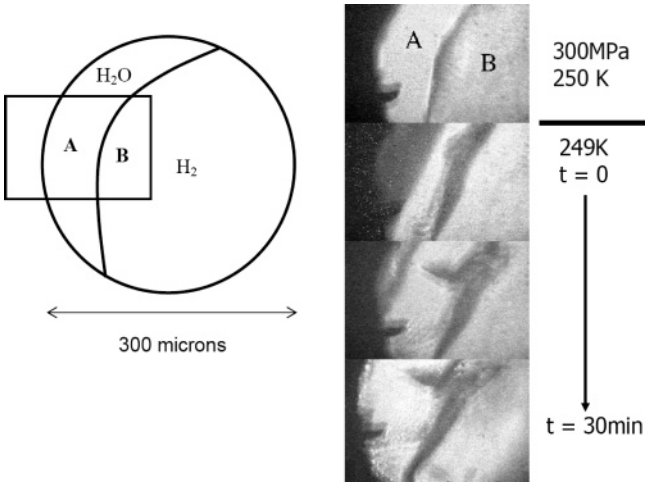

Figure 7. Synthesis of hydrogen *sII* clathrate in a diamond anvil cell. The photographs on the right side show the synthesis progress during 30 min at 249 K and 300 MPa. Parts of the figure are reprinted with permission from ref 5. Copyright 2004 by the National Academy of Sciences of the U.S.A.

studied the route suggested by Mao and Mao[18] and found that formation of the hydrogen clathrate from water and hydrogen occurs very slowly for a 1 g sample. The neutron diffraction patterns of hydrogen clathrate prepared from water at 260 K and 150 MPa have shown that the conversion of water to the clathrate phase was approximately about 30% and 70% of the clathrate content achieved after 3 and 20 h, respectively. It was also noted[44] that, in some instances, the full conversion of water to clathrate was not achieved, even after 5−10 days of synthesis. On the other hand, when ice was used as a starting material, the conversion of powdered ice with an average grain size of 0.5 mm to hydrogen clathrate hydrate was complete in less than 10 min.[44]

In summary, the hydrogen clathrate hydrate formation kinetics may be extremely slow, preventing the exact determination of the phase diagram of this new clathrate system. At this time, the tentative phase diagram shown in Figure 1 should be considered as a preliminary outline of a few experimental efforts and requires further experimental studies. The existence of slow routes for decomposition of the hydrogen clathrate may provide a means of hydrogen storage in a metastable clathrate material.

2.2. Ternary Hydrogen Hydrates

2.2.1. THF-Based Hydrates

For hydrogen clathrate, the only byproduct after release of the stored molecular hydrogen is water, making it attractive as a clean and inexpensive storage material. However, the hydrogen storage capacity has been a topic of debate. Mao et al.[4] used optical microscopy and Raman spectroscopy to estimate the hydrogen occupancy. From their results, they inferred two hydrogen molecules in each of the sixteen small dodecahedral cages and a cluster of four hydrogen molecules in each of the eight larger hexakaidecahedral cages, which is equivalent to ∼5.0 wt % molecular

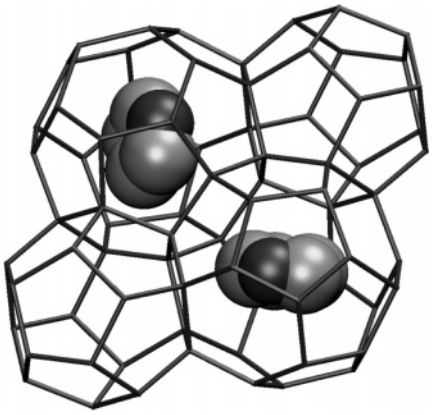

Figure 8. Clathrate structure *sII* stabilized by tetrahydrofuran (THF) molecules in large cages[45] (typically formed at high pressure and low temperature), in which host water molecules crystallize into various polyhedral cavities trapping small guest molecules (typically <9 Å).

hydrogen in the material. A neutron diffraction study[17] on deuterated samples found only one deuterium molecule in the small cages and up to four deuterium molecules (depending on $P-T$ conditions) in the large cages. Theoretical studies carried out at differing levels of accuracy have produced varying results for the hydrogen occupancy in the small cavity.[47−50] One hydrogen molecule in the small cages and four in the large would reduce the hydrogen storage capacity to ~3.8 mass %. In addition, the extreme conditions required to synthesize this material, and the very low temperatures necessary to store it, limit its potential as a practical storage material.

The addition of a promoter molecule, tetrahydrofuran (THF), was found to significantly reduce the formation pressure by a factor of 30 (from 200 to 7 MPa at 280 K) by filling the large cages and stabilizing the *sII* structure; the small cages can then be filled by molecular hydrogen.[45,46] This scheme provides a trade-off between improving synthesis or storage conditions and the reduction in hydrogen storage capacity resulting from the addition of the second guest. Udachin et al.[51] found that while He fills only 24.5% of the small cavities of the THF−He clathrate, H_2 can occupy nearly 100% of the cavities, and at higher pressure (700 MPa), it is possible for two hydrogen molecules to be accommodated in the small cavity. Florusse et al.[45] later found from gas release measurements one hydrogen molecule per small cage in the THF−H_2 clathrate, although their NMR results suggested that the small cages could potentially contain more than one hydrogen molecule. More recent high-resolution neutron diffraction studies of the THF−D_2 clathrate formed at 70 MPa suggested a single D_2 molecule occupied the small cage on average.[52] Single occupancy also gives the lowest energy for all configurations tested in molecular dynamics simulations[53] for THF−H_2 clathrates, although the unit cell configurational energies for single and double occupancy of the small cage were comparable.

Lee et al.[46] reported double occupancy of hydrogen in the small cages of the THF−H_2 clathrate formed at 12 MPa and 270 K, and they also found that they could reduce the concentration of THF so that a fraction of the large cages could be filled by a tetrahedral hydrogen cluster, and that, without sacrificing synthesis conditions, a hydrogen storage near 4 mass % could be achieved. Strobel et al.[54] used gas release and NMR methods to measure hydrogen storage capacity as a function of the initial formation pressure and THF composition. They found that as the initial formation pressure was increased to nearly 60 MPa, the hydrogen storage increased to 1.0 mass %, which corresponds to a storage capacity for nearly stoichiometric filling of large cages with THF and single occupancy of small cages with hydrogen molecules. Strobel et al.[54] did not observe hydrogen occupancy of the large cages over the entire range of pressure and THF concentrations studied, in contrast to the results reported by Lee et al.[46] The kinetics and equilibrium conditions of cage occupancy are thus questions requiring additional research.

2.2.2. Additional Ternary Systems

Investigation of the ternary and multicomponent clathrate hydrate forming systems is important for practical applications because most natural gases are mixtures of the clathrate hydrate forming gases.[55] Despite this fact, few carefully studied systems of this type are known[27] due to significant difficulties in investigation and treatment of phase diagrams of multicomponent clathrate hydrate forming systems. Generally, the data concerning these systems are limited to $P-T$ dependencies representing decomposition of the hydrate formed by the gas mixture of a given composition. Taking into account the complexity of the phase diagrams of ternary and, especially, multicomponent systems, we conclude that if the phase diagram of the multicomponent system is not studied in detail, important information may be lost. For example, the *sI* clathrate hydrates are formed in water−methane and water−ethane systems at ambient pressures. The hydrate formed in the ternary water−methane−ethane system appears to be a hydrate with *sII* structure. Analysis of the water−methane−ethane system using X-ray diffraction, Raman spectroscopy, and gas chromatography revealed clathrate structures, compositions, and cage occupancies.[56] Experimentally, hydrate structure II existed in samples formed when the gas equilibrated with hydrates was approximately 2% C_2H_6 (molar fraction) whereas both structures I (*sI*) and II (*sII*) coexisted for 12−22% C_2H_6. The structures below 2% and above 22% of C_2H_6 existed only as *sI* hydrates. Some additional information concerning the decomposition curves of the hydrates formed in the ternary systems is summarized in refs 27 and 57.

Properties of clathrate hydrates formed in ternary systems may differ significantly from those with one type of guest molecule. First of all, each type of cavity in the double hydrates may be occupied by the gas molecule with the most suitable size, which increases the packing density of the hydrate. Due to this fact, the decomposition temperatures of the double clathrate hydrates in many cases are higher in comparison with those of the clathrate hydrates of each component.

Small impurities of another gas may dramatically change the structure of the clathrate hydrate formed. The methane−propane system is given as an example. Even a small admixture of propane to methane (less when 1%) causes formation of the *sII* clathrate hydrate instead of the *sI* clathrate hydrate which is characteristic of pure methane.[58]

We have new results on the $H_2-H_2O-CH_4$ system (with H_2-H_2O and H_2-CH_4 as binary end members) (Figure 9). It was established earlier[14,59] that addition of methane to water enhances the hydrogen bonding in the water−methane framework at much lower pressures than in pure H_2O ice. We expect lower pressures and higher temperatures for the stability of hydrogen-rich end members of this ternary system

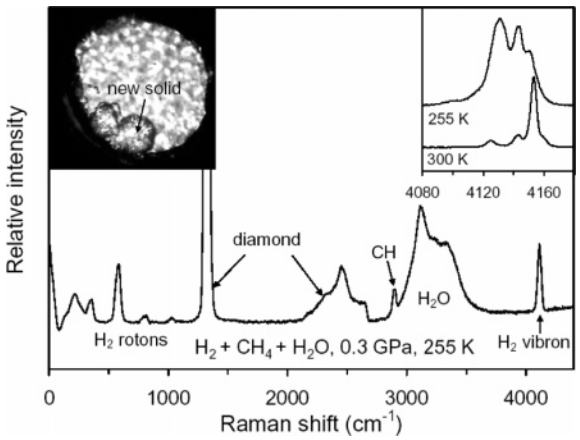

Figure 9. Preliminary results on the $H_2-H_2O-CH_4$ system showing a compound that forms at 300 MPa and 250 K. The hydrogen content in this compound is still not determined; the phase diagram is under investigation. The new solid does demonstrate that there is a potential hydrogen storage material in this ternary system.

due to the enhanced hydrogen bonding. Our recent results on a hydrogen−water−methane system demonstrate that a new solid forms at 300 MPa and 255 K.

The Raman spectra of the new solid in Figure 9 show C−H vibrations around 2900 cm^{-1}, O−H bands of the water framework between 3000 and 3250 cm^{-1}, and both H_2 rotons and a H_2 vibron. The inset in Figure 9 shows the details of the vibron Raman spectra at 255 K and 300 MPa; the low-frequency shift of the vibron frequencies at 255 K is characteristic for hydrogen enclathration. Thus, we expect that the new phase is possibly a clathrate structure. Future structural studies will provide unambiguous identification of the new phase. Available theoretical and experimental information on the extensively studied H_2O-CH_4 binary system may be used to optimize the new ternary compound for hydrogen storage.[27]

Future studies of the ternary H_2-H_2O-X system with a third molecular component based on second row elements of the Periodic Table may prove important. For example, systems based on simple molecules may be examined, including CO_2, NH_3, diluted HF, unsaturated hydrocarbons, and similar molecular compounds. It is clear that one H_2 molecule is too small to stabilize a 7 Å dodecahedral cage of the conventional clathrates, an effect that decreases the stability of the pure-hydrogen clathrate at low hydrogen content. However, understanding of the structure and bonding of the hydrogen molecules in the clathrate hydrate provides important insight into increasing clathrate stability. Substitution of the H_2 molecule in the small cage by the "size appropriate" guest entities would result in a drastic increase in clathrate structure stability. Thus, mixed clathrates could be stable under moderate pressure and room temperature, which would make these compounds suitable for the application as hydrogen storage materials.

The purpose of including additional molecules in the clathrate hydrate structure is to enhance their stability as a function of temperature and pressure. The type of guest molecule significantly affects the decomposition temperature, e.g., at 0.1 MPa, 145 K for H_2 clathrates,[4] 230 K for Ar, and 284 K for ClO_2.[60] However, additional guest molecules will add mass and also take away a fraction of the available storage volume. Future research should be focused on identifying specific guest molecules, for which the increased stability will outweigh the unwanted side effects of adding extra mass. The addition of new guest molecules also offers another intriguing new possibility because they can, in principle, lead to the formation of different clathrate structures (e.g., *sH*, which has large cages with 5.7 Å diameter compared to 4.7 Å in *sII*) and could therefore accommodate more hydrogen.

2.3. Outlook for More Complex Structures

2.3.1. Beyond Cubic

At present, only the *sII* clathrate structure is known to accommodate hydrogen at low pressures (below 300−400 MPa): in the binary H_2-H_2O system and in the ternary $H_2-THF-H_2O$ system. The clathrate structure *sH* and more complex structures having large $5^{12}6^8$ cavities potentially may hold more hydrogen than the *sII* structure, since the $5^{12}6^8$ cage has been predicted to hold up to five argon atoms.[61] Even more complex structures are possible[22] when combining together a few water cages as shown in Figure 2.[62,63] The review by Dyadin and Udachin[22] gives an extensive list of possible clathrate structures. For example, they describe multiple, or combined, cages, formed from a few elementary building blocks (Figure 2). These multiple cages may hold larger molecules than the largest *I*-type ($5^{12}6^8$) cage in Figure 2. The review of the structure, stoichiometry, and stability of the polyhydrates of tetraalkylammonium salts and trialkylamine oxides given by Dyadin and Udachin[22] describes the effects of size and configuration of the hydrophobic part of the guest molecule and its ability to undergo hydrophilic interaction with the framework. A comparative analysis of the structures in relation to those of the ideal gas hydrates is also presented in that review. Dyadin and Udachin[22] elaborate on the guest molecule size- and shape-related reactivity in these systems and analyze the ability of water to construct frameworks with appropriate cages. This information forms a basis for future molecular engineering approaches to hydrogen storage in complex clathrates. The example of such an approach is given in the next subsection.

2.3.2. Semiclathrates

The family of inclusion compounds is very diverse and is not limited to the simplest cubic and hexagonal structures (Figures 3−5). Water molecules can encage not only hydrophobic molecules but also larger molecules which have hydrogen-bonding abilities in their structural units. The larger molecule can attach to the water molecules' network by hydrogen bonding and fit into complex composite (or multiple) cages with part of their walls removed and replaced with the active part of the guest molecule. The remaining empty cages can be used to store hydrogen. This approach has been recently reported[64] to provide 0.2 mass % of hydrogen storage in a semiclathrate hydrate of tetra-*n*-butylammonium bromide (TBAB). TBAB forms the semiclathrate hydrate crystal, $C_{16}H_{36}NBr \cdot 38H_2O$, under atmospheric pressure.[65] TBAB cations are disordered and are located at the center of four cages, viz. two tetrakaidecahedra and two pentakaidecahedra in ideal cage structures, while all the dodecahedral cages are available for inclusion of appropriate guest molecules.[65]

2.3.3. Molecular Hydrogen + Hydrocarbon Compounds (Dual Fuel)

Recent work has demonstrated that storing molecular hydrogen in hosts of simple molecular materials such as H_2O,

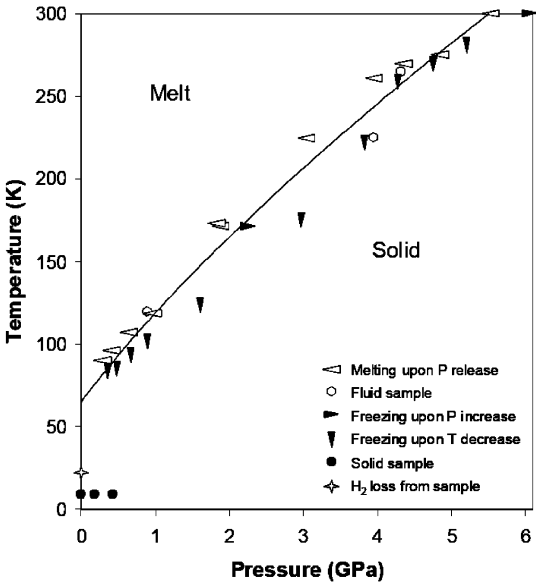

Figure 10. Melting curve of $(H_2)_4CH_4$.[67] Melt refers to a fluid mixture of H_2 and CH_4. This material demonstrates the potential of hydrogen plus simple hydrocarbon systems, and suggests the search for novel hydrogen-rich compounds with other alkanes and hydrocarbons.

CH_4, NH_3, CO_2, and other larger molecules provides an attractive alternative method for hydrogen storage. A great variety of gas−ice molecular compounds have been synthesized by varying the $P-T$ conditions and the chemistry of the gases and ices,[34−36] but systems involving molecular hydrogen have been scarcely studied. Two binaries, H_2-H_2O[14] and H_2-CH_4,[13] were previously investigated at high P and 300 K for planetary[66] and physical chemistry interest, resulting in the synthesis of a myriad of hydrogen-rich, crystalline compounds. Some of these compounds have already been mentioned in a previous discussion; we give a more complete list below: $H_2(H_2O)_6$ (23 g/L hydrogen), which is stable above 700 MPa,[14,59] "filled ice" $H_2(H_2O)$ (110 g/L hydrogen), which is stable above 2,200 MPa,[14] and $H_2(CH_4)_2$, $H_2(CH_4)$, $(H_2)_2(CH_4)$, and $(H_2)_4(CH_4)$, which are stable between 4,500 and 8,000 MPa.[13] These pressures are, however, too high; the hydrogen-bearing solids must be brought to near ambient P to be of practical interest to hydrogen storage.

As described above, other intriguing findings have been obtained in investigations of the H_2-CH_4 binary system. The $(H_2)_4(CH_4)$ compound contains 33.3 mass % molecular hydrogen (i.e., not counting the hydrogen in CH_4).[13] The stability field of $(H_2)_4(CH_4)$ extends to 5,000−6,000 MPa at 300 K, and it becomes the only molecular compound between H_2 and CH_4 at 160 K and 1,000 MPa. The low-pressure stability boundary of $(H_2)_4(CH_4)$ was found to be 300 MPa at 77 K; the melting curve of this compound was measured to nearly ambient pressure (Figure 10).[67] Although the melting curves of $(H_2)_4(CH_4)$ and pure hydrogen are similar above 1 GPa, they differ significantly at lower P, where the application to hydrogen storage is relevant. The $(H_2)_4(CH_4)$ solid is stabilized to 40 K higher T than pure hydrogen at the same P.

Van der Waals compounds of H_2 and simple hydrocarbon molecules can be used as a dual fuel by releasing molecular hydrogen as the primary fuel and then consuming the remaining hydrocarbon as the secondary fuel. Alternatively, the hydrocarbon can be recovered for the next cycle of hydrogen storage, providing an environmentally friendly solution. Only two systems, hydrogen−octane and hydrogen−methane systems, have been investigated. At high P, hydrogen forms a series of crystalline molecular compounds with methane.[13] At high pressure, hydrogen also forms compounds with molecules that are inert at ambient conditions. For example, hydrogen combines with argon to form $Ar(H_2)_2$, which contains 9.2 mass % hydrogen;[15,68] it is just one of a number of high-pressure compounds that have not been studied in the context of a hydrogen storage material but may hold promise.

The stability of H_2O-based clathrates is limited by the strength of hydrogen bonding in the clathrate cages. Group-IV element clathrates (Si, C) with strong covalent bonding could serve as carbon-based clathrates. Carbon clathrates are predicted to have many fascinating properties,[69] including high-T_c superconductivity;[70] however, the reported experimental findings are limited to the hexagonal form of the C_{36} clathrate structure.[71] Simultaneous synthesis and characterization of clathrate materials of silicon (which have been known since 1965[72]) and carbon at high $P-T$ conditions in a hydrogen pressure medium could be done, with subsequent quenching of the materials to ambient conditions. The reported fullerene-based cuboid-C_{60} clathrate-like structure[73] could be a potential compound for hydrogen storage. For completeness, we would like to mention here silica clathrates.[74,75]

3. Experimental Probes

3.1. Neutron Scattering

3.1.1. Structure

A hydrogen molecule contains only two electrons and thus is hard to probe with X-rays (since the scattering power by X-rays is related to the square of the atomic number). In contrast, neutrons interact with the nucleus rather than the electron cloud, and the scattering power is not as directly dependent on atomic number. Neutron diffraction is a well suited technique for studying the structure and dynamics of hydrogen-containing materials, and it is quite sensitive to the position of hydrogen and its isotopes (especially deuterium). Neutrons are also more penetrating than X-rays, and one can probe samples in more complex sample environments (e.g., high-pressure vessels, refrigerators and furnaces, etc.). However, fluxes from neutron sources are much lower than those from synchrotron X-ray sources, and neutron diffraction requires much larger samples.

The moderate P and low T stability of the hydrogen storing molecular compounds means a high-pressure low-temperature fluid/gas aluminum cell (which has much larger sample volumes than diamond anvil cells) can be used to perform *in-situ* neutron diffraction. Aluminum is used to construct the pressure cell, because it has a small cross section of neutron scattering and maintains reasonably high strength under hydrogen pressures. To avoid incoherent scattering of hydrogen, which contributes to the backgrounds of diffraction patterns, deuterated samples are used. For the study by Lokshin et al.,[17] the deuterated clathrate was synthesized from a mixture of D_2 and D_2O, and its stability was monitored as a function of P and T. The hydrogen clathrate was obtained under 2.2 kbar of D_2 pressure in the temperature range 200−270 K, and neutron data were collected during cooling from 200 to 40 K and during heating from 40 to 200 K at ambient

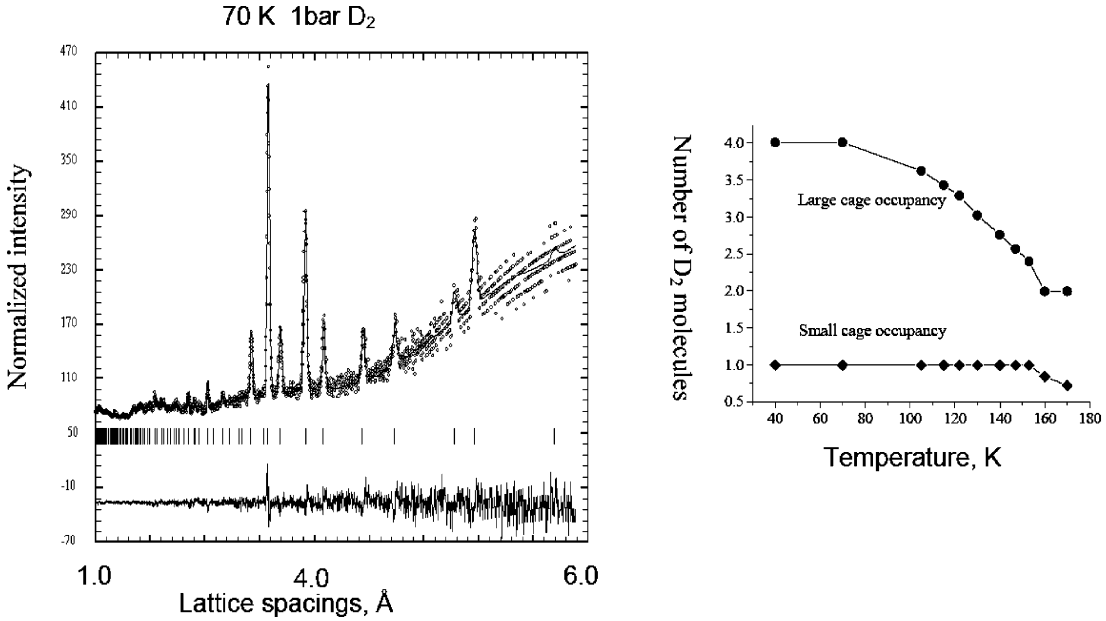

Figure 11. Neutron diffraction data for the deuterated clathrate synthesized from a mixture of D_2 and D_2O.

pressure. The number of D_2 molecules and their distribution in the cages was found to vary systematically with P and T (Figure 11). Below 50 K, the guest D_2 molecules are localized, where one D_2 occupies the small cage and four D_2 molecules are in the large cage arranged in the tetrahedral geometry with a D_2-D_2 distance of 2.93(1) Å. Interestingly, the four D_2 molecules in the large cages are oriented toward the centers of the hexagons formed by the framework water molecules, presumably due to the energetic need of minimizing their electrostatic repulsion. On the other hand, the distance between the four tetrahedrally arranged D_2 molecules (2.93 Å) is very small—much shorter than that in the solid hydrogen at low T (3.78 Å).[76] With increasing temperature, D_2 molecules become delocalized, as represented by a uniform distribution in terms of their scattering densities on the surface of a sphere, and the number of D_2 molecules in the large cage gradually reduces to two as temperature is allowed to increase to 163 K at ambient pressure (Figure 11). In contrast, the occupancy of the small cage was found to be constant at one D_2 molecule per cage throughout the temperature range.

In summary, neutron scattering provides valuable quantitative information on the enclathration of deuterium under different temperature and pressure conditions. Such information would be quite difficult to obtain by existing gravimetric techniques, since they are not well suited for the low temperatures required for hydrogen clathrate at low pressures.

3.1.2. Phonon Density of States

The measurements of the incoherent inelastic neutron scattering (IINS) are usually performed with energy resolution of about 0.1 meV—see, e.g., Tse et al.[79] and Itoh et al.[77,78] In such measurements the dynamic scattering factor $S(Q,\omega)$ is obtained. The scattering law is connected to the generalized susceptibility $\chi''(Q,\omega)$ via $S(Q,\omega) = 1/\pi[1 + n(\omega)]\chi''(Q,\omega)$ were $n(\omega)$ is the Bose−Einstein thermal population factor. When comparing different substances, the phonon density of states (PDOS) is a particularly useful quantity. For neutrons scattered incoherently in a one-phonon process

$$S(Q,\omega) = \sum_{i=1}^{N} c_i \frac{\hbar Q^2}{2} \frac{\sigma_i}{m_i} \exp(-2W_i) \frac{F_i(\omega)}{\omega} [n(\omega) + 1]$$

with partial densities of states

$$F_i(\omega) = \frac{1}{3N} \sum_{j\boldsymbol{q}} |e_i(j,\boldsymbol{q})|^2 \delta[\omega - \omega(j,\boldsymbol{q})]$$

and the Debye−Waller factors

$$W_i(Q) = \frac{\hbar Q^2}{2m_i} \int_0^\infty \frac{F_i(\omega)}{\omega} [2n(\omega) + 1]\, \mathrm{d}\omega$$

where c_i are the concentrations of the different atom types. The index j numbers the phonon branches with frequencies $\omega(j,\boldsymbol{q})$ and eigenvectors $\boldsymbol{e}(j,\boldsymbol{q})$. It is thus possible to extract a generalized form of the density of states (GDOS) from the coherent neutron spectra (using the incoherent approximation[79]) in which the contributions of the different atoms to the PDOS are weighted by the scattering powers σ_i/m_i.

Inelastic neutron scattering on different types of clathrates (Ar, Xe, O_2, and N_2) as well as MD simulations for the mode assignment were performed by Itoh et al.[78] It was found[78] that the spectral features of two intense peaks at about 6.5 and 10.5 meV are distinct from the spectrum of hexagonal ice and provide a fingerprint of the open-cage structure of the host lattice. From a comparison of the experimental N_2 contributions to the spectrum and the results of MD simulations, they assigned N_2 internal modes in small and large cages. They also predicted characteristic low-frequency modes of N_2 molecules in doubly occupied N_2 clathrate by MD simulations. From their INS experiments and MD simulations, it became clear that clathrates not only have the expected different spectral features of the guest modes but also exhibit a variable coupling of the guest modes with the host lattice. For instance, by comparing the low-frequency

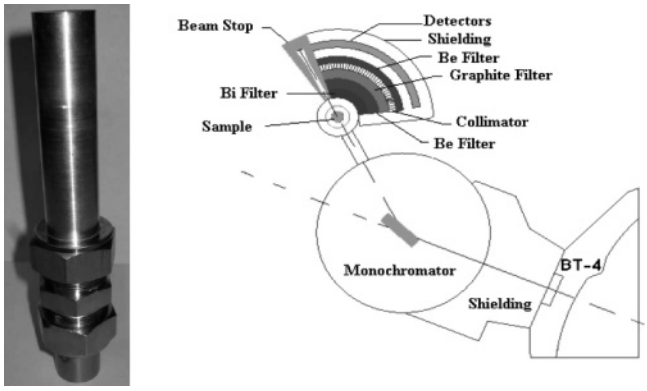

Figure 12. Neutron INS cell and FANS setup[133] at NIST. Cell design based on Leão, modified for slightly higher pressures. Both the available copper and graphite monochromators were used to get a spectrum from 5 to 160 meV (40−1300 cm^{-1}).

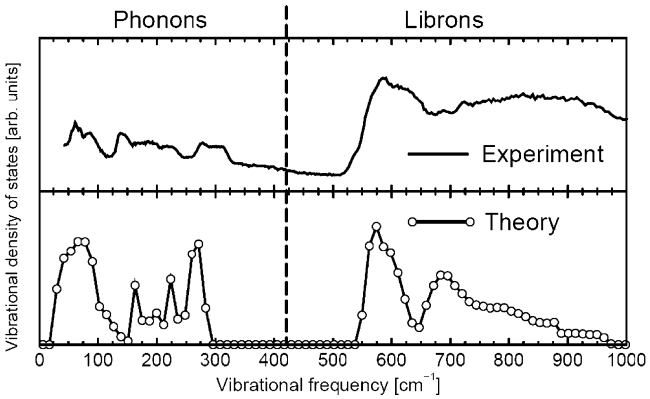

Figure 13. Comparison of neutron inelastic scattering data measured for hydrogen clathrate (H_2+H_2O+THF) with the calculations for H_2O clathrate type *sII* cages. Calculations reproduce the librational modes of H_2O above 500 cm^{-1} (∼70 meV) and the cage deformational modes (phonons) below 300 cm^{-1} (∼40 meV). The experimental data are from T. Jenkins et al., ref 134.

modes in large cages, Xe modes were found shifted and have higher anharmonicity than N_2.

INS scattering studies of hydrogen clathrate have been performed (Figure 12). The INS spectra are presented in Figure 13, along with the lattice dynamics calculations of phonon density of states. Calculations for the empty cages show the gap between the librational modes of H_2O above 70 meV and the cage deformational modes below 40 meV. The low-frequency part of the phonon band consists of vibrational modes where the clathrate cages move as a whole and get distorted at the same time. No clear distinction between breathing and translational modes can be made. We obtain good overall agreement with experiment; the distinct lower frequency and higher frequency vibrations correspond to the phonon and libron bands, respectively. The INS spectra may provide additional information if isotope shifts are analyzed. Experimentally, additional modes are observed in the experiment in the region of hydrogen rotons (20−50 meV).

The classical TIP4P force field (see section 4) was used to characterize the interaction of the water molecules in the clathrate cage. In this model, the water molecules are treated as rigid objects that interact via a short-ranged Lennard-Jones term as well as via the Coulomb potential between three point charges that are assigned to each molecule (see Iitaka and Ebisuzaki's[80] calculations of the pressure effects in the methane hydrate "filled ice" high-pressure phase). The vibrational properties of the type *sII* clathrate hydrate

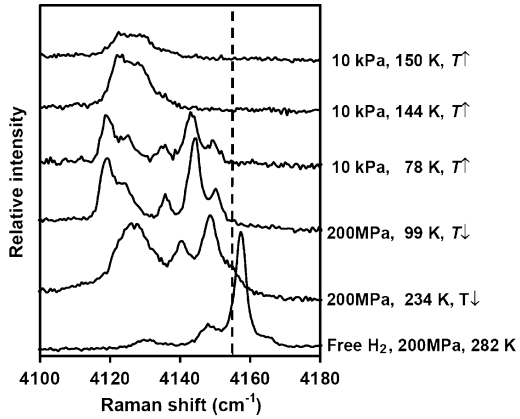

Figure 14. Raman spectra of hydrogen clathrate in the hydrogen vibron range.[4] The vertical dashed line marks $Q1(1) = 4155$ cm^{-1} for free hydrogen molecules at ambient conditions. Reprinted with permission from ref 5. Copyright 2002 by the American Association for the Advancement of Science.

structure studied with INS were compared with lattice dynamics calculations using the force field. Very good overall agreement is found for the observed phonon and libron bands (Figure 13).[81]

3.2. Raman Scattering

3.2.1. Internal Modes—Crystal Field

Mao et al.[4] used Raman scattering to characterize the hydrogen clathrate. At the formation of the clathrate, broad liquid water O−H peaks at 3000−3600 cm^{-1} transformed to sharp peaks typical of *sII* clathrates. Meanwhile, hydrogen roton peaks appeared at 300−850 cm^{-1} and vibron peaks at 4100−4200 cm^{-1} (Figure 14). The hydrogen rotons, $S_0(0)$, $S_0(1)$, and $S_0(2)$, in the clathrate were similar in frequency to those of pure hydrogen, indicating that the hydrogen molecules in clathrate cages were still in free rotational states. The H−H vibrons of the new clathrate, on the other hand, are distinct from those of other known phases in the H_2−H_2O system. The vibrons of the hydrogen *sII* clathrate appear at 4120−4150 cm^{-1} (Figure 14), which is below the dominant Q_1 vibron at zero pressure (4155 cm^{-1}). This softening arises from increased intermolecular vibrational coupling within the H_2 clusters. Attractive interactions between the hydrogen molecules and the host (even transfer of electron density) could result in additional stabilization of the clathrate without confining pressures. Once the hydrogen *sII* clathrate was synthesized at 200 MPa, it showed remarkable stability (or metastability) and persisted to 280 K upon warming. Along another $P-T$ path, it was cooled to 78 K, and then pressure was released completely. The sample at 78 K was exposed to the N_2 gas pressure (10 kPa) in the cryostat, and the clathrate remained. The vibron spectra (Figure 14) of the clathrate displayed two groups of multiplets of nearly equal intensities, supporting the assignment of two equal populations of hydrogen molecules in eight $H(5^{12}6^4)$ and sixteen $D(5^{12})$ cages. Mao et al. tentatively assigned the lower frequency group at 4115−4135 cm^{-1} to the loosely fitted tetrahedral molecular cluster in the *H* cage and the higher frequency group at 4135−4155 cm^{-1} to the bimolecular cluster ordered in the *D* cage. When warming up from 78 K at 10 kPa, the higher frequency vibrons gradually vanished above 115 K while the lower frequency vibrons and the *sII* crystal structure persisted to 145 K. This observation is actually not consistent with the above peak

assignment in view of the neutron scattering experiments[17] (Figure 13). According to neutron experiments, the large cages start to lose hydrogen at 70−80 K, and only two hydrogen molecules are left in the large cages at 150 K, when small cages also start to lose hydrogen.

Above 145 K, the lower frequency vibrons gradually disappeared and the crystal structure collapsed, which is consistent with the neutron studies. The multiple peaks within each group contain detailed information on the extent of intermolecular vibrational coupling, including configuration information; however, the observed vibronic splittings have not yet been addressed theoretically. The lower frequency Raman peak at 4115−4135 cm^{-1} was also observed in the ternary H_2−THF clathrate system, were hydrogen should mostly occupy small cages.[45] We may conclude that existing experimental evidence supports the assignment of the lower frequency peak to the small $D(5^{12})$ cages and that multiply occupied large $H(5^{12}6^4)$ cages give rise to the group of Raman modes at 4135−4155 cm^{-1}. The issue with the relative peak intensities is more complicated, since the large cages may be occupied by less than four molecules, and the filling of small cages still remains controversial (see below in section 4 the discussion of theoretical results on this issue).

The Raman spectra of enclathrated THF molecules are relatively well understood.[82] The reorientational motion of enclathrated THF molecules, which is restricted due to van der Waals interactions with the host water lattice, is observed by Raman spectroscopy.[82] The THF ring breathing mode, which is symmetric at high temperatures, broadens significantly and becomes asymmetric at low temperature. Rough activation energy analysis using data obtained from NMR and dielectric experiments suggests that the reorientation rate of enclathrated THF molecules approaches that of the isolated molecule at about 120 K. The rapid reorientational motion of the thermally activated THF molecules at 120 K results in a symmetric Raman line shape for the ring breathing mode. The bandwidths of the uncoupled OD vibrational spectra of the host water lattice between 10 and 170 K in the THF clathrate hydrate were used to characterize the distribution of O−H---O hydrogen bond lengths.[82] They range from 2.727 to 2.810 Å at 10 K and from 2.738 to 2.825 Å at 170 K. These data are in good agreement with data collected at higher temperatures.

3.2.2. Rotational and Translational Modes

The lower frequency region of the Raman spectrum of the hydrogen clathrate including lattice modes and hydrogen rotational bands is much less studied in comparison to the H_2 vibron region (Figure 15c). The low-frequency spectra from hydrogen-rich solids (Figure 15a) are usually dominated by the rotational excitations of the hydrogen molecule. The rotational bands could be split by crystal field effects (Figure 15a).[83] The details of the interactions with the host lattice could be extracted from low-temperature Raman spectra, similar to the information on intermolecular interaction extracted from the Raman measurements on solid hydrogen.[84] Such an approach has not yet been pursued to the full extent; only the hydrogen vibron region was used for the characterization of hydrogen clathrate hydrates (see previous section).

3.3. Nuclear Magnetic Resonance

Proton nuclear magnetic resonance (NMR) spectroscopy provides information about the motion of water molecules

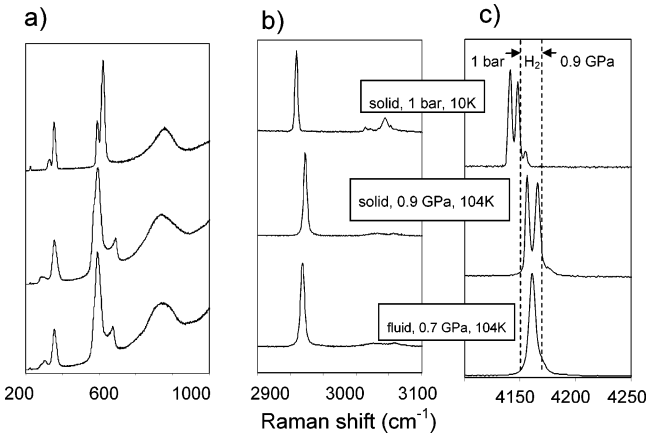

Figure 15. Raman spectra of $CH_4(H_2)_4$ in different spectral ranges. The 1 bar and 0.9 GPa (900 MPa) dashed lines in part c correspond to the hydrogen vibron positions in fluid hydrogen. (a) Rotons and translational modes region; (b) C−H stretch vibrational frequency region; (c) vibron region of the H_2 molecule.

in crystal structures.[85] At low *T*, the proton NMR analysis is sensitive in the first order to the motion of water molecules due to reorientation; the second-order contribution comes from translational diffusion.[85] ^{13}C NMR spectroscopy allows resolving the occupation of cages. For example, Ripmeester et al.[86] determined the occupancy of methane in the small and large cages of *sI* and *sII* using crosspolarization and magic angle spinning techniques.

^{129}Xe NMR spectroscopy has been used to identify ratios of Xe atoms in small and large cages, to resolve the shape of cages, to measure the kinetics of *sI*−*sII*−*sH* transitions (see ref 27). The proton (^1H) magic angle spinning (MAS) NMR was used by Florusse et al.[45] (solid-state ^1H NMR spectra of H_2/tetrahydrofuran-d_8 (H_2/TDF) hydrate). The NMR spectra showed a broad, intense resonance line with a chemical shift of 4.3 parts per million (ppm), which was present due to H_2 molecules encapsulated in this *sII* hydrate. The H_2 molecules most likely occupy only the small cages to a significant extent because the TDF molecules occupy nearly all the large cages in this *sII* hydrate.[45] Florusse et al.[45] concluded that the ^1H MAS NMR spectrum of the H_2/TDF hydrate showed no definitive evidence of multiple H_2 gas occupancy of a single small cage; however, the relatively large line width observed for its resonance line was consistent with an increase of homonuclear dipolar broadening that most likely would occur if each small cage contained more than one H_2 molecule guest.

Lee et al.[46] reported recently ^1H MAS NMR spectra of the THF−H_2 double hydrates formed at 12.0 MPa and 270 K as a function of concentration of THF. The NMR samples were prepared from deuterated water (D_2O, 99.9 atom % D) and THF (THF-d_8, 99.5 atom % D). The chemical shifts of D_2O and THF-d_8 were identified from the NMR spectrum of THF-d_8 hydrate. The samples were transferred to an NMR rotor and analyzed at 1 bar and 183 K. As the hydrate is not absolutely stable under these conditions, quantitative spectra could not be obtained because of ongoing decomposition, although a consistent picture was constructed from the spectra that showed several characteristic features. The distribution of hydrogen molecules in both cages of *sII* was found to depend on temperature and pressure of synthesis. The NMR spectra showed a broad line at 4.3 ppm (similar to Florusse et al.[45]) which was attributed to H_2 in the small cavities of the double hydrate. Lee et al.[46] further suggested that full

loading of the small cavities of THF·17H_2O with hydrogen ($2H_2$ per small cage) resulted in a storage capacity of 2.1 mass % H_2. Lee et al.[46] observed that when the concentration of THF reaches 1 mol %, a new ^{1}H NMR line appears at 0.15 ppm., which continues to grow with decreasing THF concentration. Considering the other experimental evidence for the increased loading of the sample, they assigned this peak to H_2 clusters in the large cages. Strobel et al.[54] repeated the synthesis conditions reported by Lee et al., but they did not confirm the double occupancy of small cages or any observable occupancy of the large cages. They also did not see any NMR signal from ^{1}H NMR in large cages. The controversy in these two studies was attributed to inadequate use of the Raman signal in the hydrogen vibron region to quantify the amount of stored hydrogen. According to Strobel et al.,[54] the maximum amount of hydrogen stored in this binary hydrate was about 1.0 wt % at moderate pressure ($<$60 MPa) and is independent of the initial THF concentration over the range of conditions tested. The accurate determination of the H_2 occupancy in the small cage of the hydrate under different *P*, *T* thermodynamic conditions is the key to establish whether H_2 hydrate will be a suitable medium for H_2 storage.

Okuchi et al.[87] measured recently the hydrogen NMR signal in the filled ice. With *in situ* proton NMR spectra, T_1^{-1} and T_2^{-1} of filled-ice hydrogen hydrates at high pressure reveal fast translational motion of the H_2 molecules within the ice frameworks. The NMR spectra to 3.6 GPa gave surprisingly narrow resonances of the H_2. Pressure effects on T_1^{-1} and T_2^{-1} of the H_2 indicate that molecular rotation and diffusion contribute together to the relaxation, from which correlation times were determined. Liquidlike diffusion with little pressure sensitivity was deduced, indicating the ice framework allows active guest translation even in compressed states.

3.4. Thermal Conductivity and Heat Capacity

The hydrogen clathrate discovery is so recent that there are few published data on the thermophysical properties of this compound. However, we would like to discuss briefly some recent results on clathrates of noble gases which are related to complex guest dynamics in clathrate cages, which is also expected to be the case for hydrogen clathrates. Both *sI* and *sII* structure types contain 80% of hydrogen-bonded water molecules; thus, many properties of these clathrate structures resemble those of ordinary ice Ih. This, however, is not true for the thermal conductivity κ, which is unusually low and displays a temperature dependence similar to that of glasses,[88,89] despite the crystalline character of the clathrate hydrates. At least two different qualitative models have been proposed to explain the unusual thermal conductivity: (i) the large unit cell is leading to a limited phonon mean free path, and (ii) a coupling between the guest and host vibrations in the low-frequency region leads to effective phonon scattering (see Tse and White[90] and references therein). Recently, the guest−host coupling was confirmed experimentally in inelastic incoherent neutron scattering experiments on structure type *sI* xenon hydrate.[77,91] Very recently, the anharmonic mixing of host and guest vibrations was confirmed for the *sII* krypton hydrate.[92] The unusual thermal conductivity of clathrate hydrates is due to extensive mixing of localized anharmonic "rattling" motions of guest atoms or molecules with the host lattice phonons. This was shown by Tse et al.[92] by the use of two complementary techniques. First, the inelastic incoherent neutron scattering data imply that there is a very strong coupling between the guest and icelike lattice vibrations, as seen from the distinct features in the data resulting from the effect of the guest vibrations on the cage dynamics.[92] Second, nuclear resonant inelastic scattering[93] provides complementary data that confirm the significant anharmonic character of the guest-atom vibrations. Tse et al.[92] concluded that strong anharmonic coupling of lattice and guest vibrational modes (both translational and librational, such as the clathrate hydrate of tetrahydrofuran) is responsible for the scattering of heat-carrying lattice phonons leading to glasslike anomalies in the thermal conductivity. These authors further imply that in general this mechanism is analogous to that in crystalline polymers or supramolecular solids (for example, Dianin's compounds[94]), where low-energy librational motions (even without the presence of guests) have also been shown to couple strongly with the acoustic waves, thus diminishing the thermal conductivity. Future INS experiments and measurements of thermal conductivity may help to establish the degree of anharmonic coupling between the host clathrate lattice and enclathrated hydrogen molecules and provide constraints on hydrogen molecule interactions within the clathrate cages.

Measurements of the heat capacity of clathrates are often used to deduce the contribution of the rotational degrees of freedom of guest molecules and interpreted in terms of hindered rotations at low temperature. Handa and his coworkers at National Research Councel (Canada) carried out calorimetric studies at ambient and high pressures.[95−99] The field of calorimetric studies in clathrates is enormous and deserves a separate review. We describe below a few studies which may be relevant for understanding of the THF clathrate hydrate which has been widely used for increasing the stability of the hydrogen clathrate. The measurements of the heat capacity of tetrahydrofuran (THF) clathrate hydrate from $T = 17$ to 261 K were reported by White and MacLean.[100] The results were consistent with free or nearly free rotation of the THF guest molecules in the host lattice at temperatures above 120 K. At lower temperatures, this rotation becomes hindered, but the reduction of rotational freedom is gradual and does not result in a phase transition. The hexagonal ice is a good model for the empty lattice above 120 K but not below this temperature. The authors suggested that the observed difference in heat capacity reflects the role of the long-range order in the determination of the low-temperature lattice heat capacity. From the heat capacity of the THF molecule, the barrier to rotation for the THF guest molecule was calculated to be 3.5 kJ mol^{-1}, in good agreement with that determined by other methods.

Pure liquid water freezes to produce at least eight forms of ice from the liquid; at higher pressures, it freezes to ices III, IV, V, VI, VII, and XII, and at ambient pressure, it freezes to hexagonal and cubic ices depending upon the size of the droplets and films. Also, when its amorphous state produced by collapsing hexagonal ice at 77 K is heated, it crystallizes to two other ices, II and IX, which do not form by cooling liquid water. In the presence of small molecules (e.g., Ar, N_2, CO_2, SF_6, methane, acetone, dimethyl ether, ethylene oxide, tetrahydrofuran, and cyclopentane), liquid water crystallizes into one of three types of clathrates with exceptionally large unit cells (Figures 3−5). The guest molecules stabilize the cagelike structures, and the strength of interaction between the H_2O and the guest molecule in the cagelike structures determines the stability of the clathrate

hydrate, its structure, and its formation conditions. The O−O−O angles in all the three crystal structures deviate from the ideal tetrahedral value, and the O−H −O hydrogen bonds are nonlinear. Tombari et al.[101] reported a thermodynamic study of the formation of tetrahydrofuran clathrate hydrate by explosive crystallization of water-deficient, near stoichiometric, and water-rich solutions, as well as of the heat capacity, C_p, of supercooled tetrahydrofuran−H_2O solutions and of the clathrate hydrate, THF liquid, and supercooled water and the ice formed on its explosive crystallization. In explosive freezing of supercooled solutions at a temperature below 257 K, THF clathrate hydrate formed first. The nucleation temperature depends on the cooling rate, and excess water freezes on further cooling. The clathrate hydrate melts reversibly at 277 K, and C_p increases by 770 J/(mol K) on melting. The enthalpy of melting is 99.5 kJ/mol, and the entropy is 358 J/(mol K). The molar C_p of the empty host lattice is less than that of the ice, which is inconsistent with the known lower phonon frequency of H_2O in the clathrate lattice. Analysis shows that the C_p values of THF and ice are not additive in the clathrate. The C_p of the supercooled THF−H_2O solutions is the same as that of water at 247 K, but it is less at lower temperatures and greater at higher temperatures. The difference tends to become constant at 283 K. There is a considerable effect of the guest molecules on the thermodynamics of the host lattice. The heat capacity per mole of H_2O in the host lattice determined after subtracting the heat capacity of THF is less than that of ice. The heat capacity of stoichiometric and near stoichiometric THF−water solutions at 253 K is the same as that of supercooled water. It is higher at higher temperatures, and the difference tends to approach a plateau value of ca. 8 J/(mol K) at 283 K. It is lower at temperatures below 253 K, decreasing rapidly with further supercooling. These features seem to indicate a continuous change in the role of THF in decreasing the vibrational and the configurational contributions to the heat capacity of water by changes in the hydrogen bonding.

In summary, kinetic (thermal conductivity) and thermodynamic (heat capacity) properties of clathrates provide valuable information on complex guest dynamics and bonding in clathrate cages. Such studies are highly desirable for hydrogen clathrates, for both hydrogen- and deuterium-based clathrates. The isotope-dependent properties may provide valuable information on quantum effects in hydrogen clathrates.

4. Theoretical Developments

The mechanisms involved in molecular storage are similar but not identical to physisorption mechanisms and are governed mostly by van der Waals (dispersion) intermolecular interactions and stronger forces holding together the host framework (e.g., hydrogen bonding). Detailed experimental studies of stable molecular structures by X-ray and neutron scattering and determination of their characteristic vibrational spectra by neutron scattering, Raman, and IR spectroscopy are necessary to establish the hierarchy of molecular forces governing the retention of hydrogen and to optimize the materials for practical applications. Theoretical calculations provide further insight and guidelines for development of hydrogen-storage materials tailored to the needs of a hydrogen-based economy. The range of molecular forces used for hydrogen storage matches those of biological systems. This approach establishes routes for producing novel hydrogen-rich molecular compounds for hydrogen storage; as such, the clathrate chemistry may hold enormous potential for commercialization and practical use in a hydrogen-based economy of the future.

Given the structural complexity of the proposed materials (and clathrates in particular), theoretical work should rely on a combination of different computational techniques that can balance the system size and the accuracy needed. One can employ classical molecular dynamics based on potential models, which allows study of the dynamics of large systems such as the *sII* clathrate structure using on the order of 1000 molecules.[102] As an intermediate method, one can use density functional theory to determine ground state properties of materials on the one hand but also to study the dynamics of systems with up to 200 atoms. Finally, one can resort to advanced quantum chemistry methods that can accurately describe dispersive interactions but do not provide us with a dynamical description. The complete theoretical description is usually based on a combination of different techniques including density functional theory (DFT), molecular dynamics (MD), and similar approaches. However, the first successful theoretical description of clathrates was a thermodynamic description by the semiempirical model of van der Waals and Platteeuw,[12] which considered clathrates as a solid solution of water and gas.

4.1. Semiempirical Models

4.1.1. Extensions of van der Waals–Platteeuw Theory

Early studies by von Stackelberg and his school[60] succeeded in determination of the X-ray diffraction patterns of a number of clathrate hydrates. Almost simultaneously, Pauling and Marsh[103] determined the crystal structure of chlorine hydrate. All clathrate hydrates were suggested to have cubic structures (*sI* and *sII*) in which the guest gas molecules are situated in cavities formed by a framework of water molecules held together by hydrogen bonds. (At present, hexagonal, orthorhombic, and more complex clathrate structures are known.[22]) A common feature of all clathrates is a host lattice, which is thermodynamically unstable by itself. The inclusion of guests into cavities stabilizes the clathrate structure. Judging from the structural considerations, guests and host lattice interact by weak van der Waals forces.[6] Given the weak interaction, it seems natural then to regard a clathrate as a solid solution of the second component in the metastable host lattice, and a thermodynamic model along these lines was generalized and elaborated by van der Waals and Platteeuw in 1959.[12] In this model, the empty host lattice is considered as a "solvent". All molecules which fit into the cavities will be able to stabilize the host lattice, unless they show a specific chemical reaction with the solvent molecules.

The van der Waals and Platteeuw theory, and all of its subsequent derivatives, is based on four main assumptions: [12] (i) cages contain at most one guest, (ii) the guest molecules do not interact with each other, (iii) the host lattice is unaffected by the nature or number of guest molecules present, and (iv) classical statistics is valid. Most of these assumptions are clearly violated in the case of multiple occupancy of clathrate cages by gas atoms. The extension of the van der Waals and Platteeuw model for ternary systems was proposed by Lunine and Stevenson.[104] Some groundwork for improved theory has been performed by Dyadin and Belosludov. They showed how a nonideal solution theory

can be formulated to account for the guest−guest interaction.[105] Belosludov et al. have proposed a generalization of the existing theory of clathrate hydrates,[106] so that it can account for phenomena such as multiple occupancy of individual cages and mutual guest−host couplings and guest−guest interaction. Their new model takes into account the influence of guest molecules on the host lattice. With this model, Belosludov et al. have modeled structural, dynamical, and thermodynamic properties of ices and different hydrates at high pressures and over a range of temperatures. The authors also investigated the influence of guest molecules (argon, methane, and xenon) on the host lattice of hydrates of cubic structures *sI* and *sII*. The results of these calculations agree with known experimental data. However, they did not analyze the multiple occupancy scenario in their work. A generalization of the van der Waals−Platteeuw (vdW-P) statistical thermodynamic model of clathrate hydrates was also formulated by Tanaka et al.,[107−110] particularly in application to multiple filling of the clathrate cages in argon.[111] While double occupancy is relatively easy to handle, further extension to multiple occupancy is made by considering indistinguishable guest molecules in a single cage, and the numerical burden becomes increasingly heavier.[111] Since this method requires explicit models to treat guest−guest interactions, it becomes comparable to less empirical methods in complexity.

The hydrogen clathrate has not been approached yet with these thermodynamical models. The theoretical treatment for the hydrogen clathrate has been performed by molecular dynamics and first-principle methods, which are reviewed below.

4.1.2. Model Potential and Molecular Dynamics Calculations

Classical molecular dynamics with predefined force fields is one of the most common simulation techniques to study many-particle systems. For water clathrates, one can start from well-established potential models like TIP4P and add host−guest interactions.[112] Alternative force fields for clathrate studies have been developed.[113−115] Besides the clathrate stability, the focus of these classical simulations is on the understanding of the dynamics of the clathrate melting process and the associated hydrogen release.[32,33,49,53,61,78,92,102,114,116,117] Two recent theoretical studies of hydrogen clathrate by Alavi et al.[49] and Inerbaev et al.[50] by molecular dynamics are in general agreement with recent neutron diffraction experiments.[17] While different model potentials were used, both studies agree on the stable configuration of four hydrogen molecules in large cages and one molecule in small cages of *sII* clathrate structure. Alavi et al.[49] used an extended simple point charge model as the intermolecular potential for water and a standard Lennard-Jones potential to describe H_2-H_2 interactions. Inerbaev et al.[50] used the modified TIP4P potential for water and a modification of the Lennard-Jones potential with a softer repulsion term. Both calculations predict ∼1% volume expansion if the occupation of small cages is increased to two hydrogen molecules/cage. It was also found[50] that large cages could accommodate up to three hydrogen molecules without significant expansion; the inclusion of a fourth molecule expands the lattice by 0.5%−1%, depending on the details of the interaction potentials used.[50]

Despite the weak van der Waals interactions and almost freely rotating guests, theoretical molecular dynamics (MD) and lattice dynamics (LD) calculations have shown that in a clathrate hydrate there are collective motions between the guests and the water of the framework and strong mixing (coupling) of the localized guest and lattice vibrations.[77] It has been shown that the integrity of the clathrate hydrate framework structure against thermal excitation is derived from the *repulsive* interactions between the guest and the water.[107] The physical reason for the strong vibrational interactions is due to the small size of the hydrate cages. When the framework water is displaced from its equilibrium position, it pushes the guest atom along with it and vice versa. Therefore, the localized rattling vibrations of the guest are modulated by the host lattice vibrations. The avoided crossing between the crystal acoustic modes and the guest localized vibrations provides a convenient mechanism for the transfer of energy between the two entities. This is the cause for the resonant scattering of the heat carrying phonons proposed earlier to rationalize the experimental thermal conductivity.[90,118] It is conceivable that the thermal phonons which are carried by the low-frequency lattice vibrations may be scattered through the excitations of localized vibrations of the guest species. It is noteworthy that the localized excitation thermal conductivity model of Cahill and Pohl[119] gave a reasonable prediction on the magnitude and the temperature dependence for several clathrate hydrates. The mechanism of the coupling between the water framework and guests vibrations can also be investigated by molecular dynamics techniques. However, the calculation of the relevant intermediate scattering functions is a formidable task, as it requires many repeating unit cells to include the correct phonon dispersion.[120] A wealth of information could be obtained from neutron inelastic scattering data as described in section 3.1, if the theoretical framework[77] to treat the complex guest−host dynamics will be established for hydrogen clathrate. The fine detail of the hydrogen−hydrogen interactions in the large cage cluster awaits further experimental and theoretical work. We have recently started the MD simulations of *sII* hydrogen clathrate. An example of the calculations is shown in Figure 16.

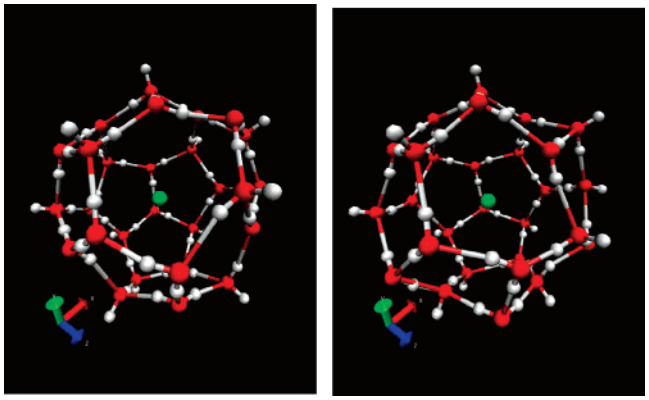

Figure 16. Two frames from a vibrational mode of a large cage in the clathrate *sII* structure. This large cage is made of 4 hexagon and 12 pentagon faces formed by 28 water molecules. The libron vibrational modes deform the cage by stretching the hydrogen bonds. The distortions shown correspond to the ∼600 cm^{-1} librational mode. The complete calculated vibrational density of states is shown in Figure 13.

4.2. First-Principle Methods

4.2.1. Ab Initio Calculations

Following the work by Iitaka and Ebisuzaki,[121] *density functional theory* (DFT) can be used to study how different guest molecules affect the stability of the clathrate cages. This technique is also useful to characterize the vibrational motion of the cage molecules and how external pressure affects the cages structure. DFT gives superior accuracy to Hartree−Fock theory and semiempirical approaches. In contrast to advanced quantum chemistry methods [second-order Møller−Plesset (MP2), coupled cluster (CC), configuration interaction (CI)], it enables fairly accurate treatment of systems with several hundreds of atoms.[122]

An estimation of the entropy and enthalpy of pure H_2 clathrates has recently been given by Patchkovskii and Tse.[47] They have given a detailed analysis of the enthalpy and entropy contributions of hydrogen guest molecules in multiply occupied small and large cages by separately considering contributions to the entropy and enthalpy from the rotation of the individual H_2 molecules in the cages and from the rotation and the vibrations of the cluster of $n$$H_2$ molecules in the clathrate cages. Patchkovskii and Tse used density functional theory (DFT) calculations[47] to model the small cage with a 20-molecule water cluster, and for large cages, a 28-molecule model cluster was constructed in a distorted T_d symmetry. To describe the host−guest interaction, they went beyond DFT and used MP2 calculation for cage geometries that were optimized with DFT. They observe that the entropy associated with the guests in the cages makes a substantial contribution to the free energy of the host−guest system and needs to be considered when the stability of different occupancies is being determined. The results of the calculations indicate that small cages are preferably occupied by two molecules. This conclusion is not in agreement with the MD calculations by Alavi et al.[49] and Inerbaev et al.,[50] predicting stable single-occupancy small cage configurations, and with experiments on neutron scattering of deuterated *sII* hydrogen clathrate.[17] In the absence of an explicit free-energy calculation similar to that of the vdWP theory, such a semiquantitative analysis will be useful in predicting the relative stability of the different occupancies in the binary clathrate THF + H_2 system.

Another DFT approach was used by Sluiter et al.[48,123] They employed the all-electron full-potential mixed-bases approach in which the electronic wave functions are expanded as a linear combination of localized atom-centered orbitals and plane waves. The localized orbitals are derived from wave functions of non-spin-polarized atoms by truncating within non-overlapping atomic spheres and subsequent normalization. Studies on H_2O have shown that the rather low (200 eV) cutoff energy gives an accurate description. This mixed-basis approach does not rely on pseudopotentials and uses local density approximation. The authors concluded that the enclathration of hydrogen molecules is based on physisorption and, therefore, density functional theory can be applied to describe the interactions in the hydrogen clathrate system. They also found, similar to the results of Patchkovskii and Tse,[47] the optimal large cage occupancy of four H_2 molecules and the small cage occupancy of two H_2 molecules, in disagreement with MD calculations[49,50] and neutron experiments.[17] However, a recent paper by Patchkovskii and Yurchenko[124] showed that if quantum effects are included, the occupancy of H_2 in the small dodecahedral cage of the *sII* hydrate will be reduced. Sebastianelli et al.[125] have calculated the ground-state properties and vibrationally averaged structural information rigorously with inclusion of quantum effects for one, two, and three *para*-H_2 and *ortho*-D_2 molecules in the small cage, using the diffusion Monte Carlo (DMC) method. They have found that, for $(H_2)_n$ and $(D_2)_n$ with $n = 1$ and 2, the ground-state energies are negative, implying that these states are truly bound and stable relative to the hydrogen molecule(s) at a large distance outside the cage (the zero of energy). These results suggest that double occupancy of H_2/D_2 in the cage is possible.

In summary, available density functional calculations suggest that small cages can accept two hydrogen molecules, as was suggested in the first report by Mao et al.;[4] inclusion of quantum effects into calculations suggests that the occupancy of H_2 in the small dodecahedral cage of the *sII* hydrate may be reduced.[124] This reduced occupancy is supported by existing MD calculations[49,50] and neutron diffraction experiments on deuterated clathrate systems.[17] At this moment, it appears that improvements are required in density functional calculations to reproduce experimental results;[17] the inclusion of quantum effects into the calculations appears to be necessary.[124−126] The effects of different isotopes should also be addressed theoretically[125] in future work, since the MD studies suggest a large contribution of zero-point motion to the stabilization energy of the clathrate.[50]

4.2.2. Theoretical Challenges

To determine the stability of novel hydrogen clathrate materials using computer simulations is a challenging task because of the large size of the *sII* unit cell with 136 water molecules. However, different groups[102,113−115] have succeeded in determining the stability using classical molecular dynamics with effective potentials, e.g., derived from the KKY model.[127] These simulations typically include $2 \times 2 \times 2$ unit cells with 1088 water molecules in periodic boundary conditions at constant pressure and temperature. The shape and the size of the simulation cell are dynamic variables. If large fluctuations from the cubic equilibrium configuration are observed, it is concluded that the structure is unstable. One also needs to incorporate hydrogen molecules as well as the new guest molecules in the simulation. The main challenge thereby is to derive potentials that can mimic dispersive interactions. This can be done by fitting results from quantum chemistry calculations. With these new effective potentials, one can then determine if certain types of guest molecules can enhance the clathrate stability. Furthermore, one can study how the guest molecule interacts with the cages and the hydrogen and can identify preferred orientations as a function of occupation of hydrogen molecules.

5. Conclusions

The suggested use of hydrates and other simple molecular solids for hydrogen storage applications[5] has received wide attention. While the potential for hydrogen storage was demonstrated in early studies,[4,5] optimization of the clathrate materials to match strict requirements for onboard storage[16] has not yet been achieved.[64] Accurate determination of the H_2 occupancy in the small cage of the hydrate under different $P-T$ conditions is central to establishing whether H_2 hydrate will be a suitable medium for H_2 storage in the *sII* clathrate.

However, several other molecular systems, carbon and silica-based clathrates, may hold promise for hydrogen storage and should not be overlooked in future studies. On the theoretical side, developments in hydrogen storage applications would benefit from the inclusion of quantum effects into the calculations. The effects of different isotopes should be also addressed[125] in future work, since the quasiharmonic lattice dynamics studies suggest a large contribution of zero-point motion to the stabilization energy of the clathrate.[50]

With the accelerating advances in static compression techniques in recent years, an increasing number of new materials have been both synthesized under pressure and recovered to ambient pressure. Recent developments suggest great potential for finding or exploiting other high-pressure materials. Low temperature hinders transition reversal and preserves high-pressure phases to near ambient pressure.[40] The ongoing research of the hydrogen storage in clathrates explores the moderately low (77−300 K) to moderately high (300−450 K) temperature range to search for new compounds capable of retaining a significant amount of hydrogen. However, the compounds that are formed at relatively high $P-T$ conditions may be decompressed at moderately low T. Similar strategies may help in the search for novel clathrate materials for hydrogen storage, albeit at higher $P-T$ synthesis conditions and with the use of various starting materials (e.g., graphite, hydrocarbons).

The theoretical work should proceed in close collaboration with the ongoing experiments, studying the same materials under comparable conditions. It will eventually lead to an accurate description of structure and bonding on the microscopic level and therefore will help to identify and characterize structural changes as a function of pressure and temperature. Also, the theoretical insight will guide the experimental exploration of novel molecular hydrogen storage materials. This is an extended and complex process given the large number of possible materials and different thermodynamic conditions. The goal of the theoretical effort will be to eliminate unlikely storage materials early on and to come up with more favorable candidates in order to make the experimental exploration more efficient.

In this review, along with discussing the status of hydrogen storage in clathrates, we briefly touched on diverse possibilities for molecular hydrogen storage in a broader class of molecular materials. We believe that the supramolecular approach holds great potential for new materials which may effectively and safely store hydrogen for future energy storage and distribution applications.

6. Acknowledgments

We acknowledge the support by DOE Grant Nos. DE-FG36-05GO15011, DE-FC03-03NA00144, DE-FG02-06ER46280, and DOE-NNSA. We acknowledge T. Jenkins and J. Leão for help with the experiments.

7. Note Added after ASAP Publication

This paper was published ASAP on September 13, 2007. Changes were made to section 2.2.1, and the paper was reposted to the Web on September 19, 2007.

8. References

(1) Dresselhaus, M. S.; Thomas, I. L. *Nature* **2001**, *414*, 332.
(2) Schlapbach, L.; Züttel, A. *Nature* **2001**, *414*, 353.
(3) Dyadin, Y. A.; Larionov, E. G.; Manakov, A. Y.; Zhurko, F. V.; Aladko, E. Y.; Mikina, T. V.; Komarov, V. Y. *Mendeleev Commun.* **1999**, 171.
(4) Mao, W. L.; Mao, H. K.; Goncharov, A. F.; Struzhkin, V. V.; Guo, Q.; Hu, J.; Shu, J.; Hemley, R. J.; Somayazulu, M.; Zhao, Y. *Science* **2002**, *297*, 2247.
(5) Mao, W. L.; Mao, H. K. *Proc. Natl. Acad. Sci.* **2004**, *101*, 708.
(6) Powell, H. M. *J. Chem. Soc.* **1948**, 61.
(7) Davy, H. *Philos. Trans. R. Soc. London* **1811**, *101*, 1.
(8) Faraday, M. *Philos. Trans. R. Soc. London* **1823**, *113*, 160.
(9) Davidson, D. W. In *Water: A Comprehensive Treatise*; Frank, F., Ed.; Plenum Press: New York, 1973; Vol. 2.
(10) Hammerschmidt, E. G. *Ind. Eng. Chem.* **1934**, *26*, 851.
(11) Deaton, W. M.; Frost, E. M., Jr. *U.S. Bur. Mines Monogr.* **1946**, *8*.
(12) Waals, J. H. v. d.; Platteeuw, J. C. *Adv. Chem. Phys.* **1959**, *2*, 1.
(13) Somayazulu, M. S.; Finger, L. W.; Hemley, R. J.; Mao, H. K. *Science* **1996**, *271*, 1400.
(14) Vos, W. L.; Finger, L. W.; Hemley, R. J.; Mao, H. K. *Phys. Rev. Lett.* **1993**, *71*, 3150.
(15) Loubeyre, P.; Letoullec, R.; Pinceaux, J. P. *Phys. Rev. Lett.* **1994**, *72*, 1360.
(16) DOE. http://www.eere.energy.gov/hydrogenandfuelcells/storage/current_technology.html, the targets for future hydrogen storage economy as defined by the Department of Energy.
(17) Lokshin, K. A.; Zhao, Y.; He, D.; Mao, W. L.; Mao, H.-K.; Hemley, R. J.; Lobanov, M. V.; Greenblatt, M. *Phys. Rev. Lett.* **2004**, *93*, 125503.
(18) Mao, W.; Mao, H. K. U.S.A. Patent 6,735,960, 2002.
(19) Bernal, J. D.; Fowler, R. H. *J. Chem. Phys.* **1933**, *1*, 515.
(20) Pauling, L. *The Nature of the Chemical Bond*; Cornell University Press: Ithaca, NY, 1948.
(21) Ripmeester, J. A.; Davidson, D. W. *J. Mol. Struct.* **1981**, *75*, 67.
(22) Dyadin, Y. A.; Udachin, K. A. *Zh. Strukt. Khim. (in Russian)* **1987**, *28*, 75.
(23) Stackelberg, M. v.; Muller, R. H. *Z. Elektrochem.* **1954**, *58*, 25.
(24) Jeffrey, G. A. In *Comprehensive Supermolecular Chemistry*; MacNicol, D. D., Toda, F., Bishop, R., Eds.; Pergamon: Oxford, 1996.
(25) Ripmeester, J. A.; Tse, J. S.; Ratcliffe, C. I.; Powell, B. M. *Nature* **1987**, *325*, 135.
(26) Dyadin, Y. A.; Bondaryuk, I. V.; Zhurko, F. V. In *Inclusion Compounds*; Atwood, J. L., Davies, J. E. D., MacNicol, D. D., Eds.; Oxford University Press: Oxford, 1991; Vol. 5.
(27) Sloan, E. D. *Clathrate Hydrates of Natural Gases*; Marcel Dekker, Inc.: New York, 1997.
(28) Davidson, D. W.; Handa, Y. P.; Ratcliffe, C. I.; Tse, J. S.; Powell, B. M. *Nature* **1984**, *311*, 142.
(29) Tse, J. S.; Handa, Y. P.; Ratcliffe, C. I.; Powell, B. M. *J. Inclusion Phenom.* **1986**, *4*, 235.
(30) Kamb, B.; Hamilton, W. C.; LaPlaca, S. J.; Prakash, A. *J. Chem. Phys.* **1971**, *55*, 1934.
(31) Petrenko, V. F.; Whitworth, R. W. *Physics of Ice*; Oxford University Press: Oxford and New York, 1999.
(32) Tse, J. S.; Klug, D. D. *Phys. Rev. Lett.* **1998**, *81*, 2466.
(33) Tse, J. S.; Klug, D. D.; Tulk, C. A.; Swainson, I.; Svensson, E. C.; Loong, C.-K.; Shpakov, V.; Belosludov, V. R.; Belosludov, R. V.; Kawazoe, Y. *Nature* **1999**, *400*, 647.
(34) Chou, I.-M.; Sharma, A.; Burruss, R. C.; Shu, J.; Mao, H. K.; Hemley, R. J.; Goncharov, A. F.; Stern, L. A.; Kirby, S. H. *Proc. Natl. Acad. Sci.* **2000**, *97*, 13484.
(35) Loveday, J. S.; Nelmes, R. J.; Guthrie, M.; Klug, D. D.; Tse, J. S. *Phys. Rev. Lett.* **2001**, *87*, 215501.
(36) Hirai, H.; Uchihara, Y.; Fujihisa, H.; Sakashita, M.; Katoh, E.; Aoki, K.; Nagashima, K.; Yamamoto, Y.; Yagi, T. *J. Chem. Phys.* **2001**, *115*, 7066.
(37) Lobban, C.; Finney, J. L.; Kuhs, W. F. *Nature* **1998**, *391*, 268.
(38) Chou, I.-M.; Blank, J.; Goncharov, A. F.; Mao, H. K.; Hemley, R. J. *Science* **1998**, *281*, 809.
(39) Hemley, R. J.; Ashcroft, N. W. *Phys. Today* **1998**, *51*, 26.
(40) Eremets, M. I.; Hemley, R. J.; Mao, H.-K.; Gregoryanz, E. *Nature* **2001**, *411*, 170.
(41) Chen, Z.; Strauss, H. L.; Loong, C.-K. *J. Chem. Phys.* **1999**, *110*, 7354.
(42) Strauss, H. L.; Chen, Z.; Loong, C.-K. *J. Chem. Phys.* **1994**, *101*, 7177.
(43) Klotz, S.; Besson, J. M.; Hamel, G.; Nelmes, R. J.; Loveday, J. S.; Marshall, W. G. *Nature* **1999**, *398*, 681.
(44) Lokshin, K. A.; Zhao, Y. *Appl. Phys. Lett.* **2006**, *88*, 131909.
(45) Florusse, L. J.; Peters, C. J.; Schoonman, J.; Hester, K. C.; Koh, C. A.; Dec, S. F.; Marsh, K. N.; Sloan, E. D. *Science* **2004**, *306*, 469.
(46) Lee, H.; Lee, J.-W.; Kim, D. Y.; Park, J.; Seo, Y.-T.; Zeng, H.; Moudrakovski, I. L.; Ratcliffe, C. I.; Ripmeester, J. A. *Nature* **2005**, *434*, 743.

(47) Patchkovskii, S.; Tse, J. S. *Proc. Natl. Acad. Sci.* **2003**, *100*, 14645−14650.
(48) Sluiter, M. H. F.; Adachi, H.; Belosludov, R. V.; Belosludov, V. R.; Kawazoe, Y. *Mater. Trans.* **2004**, *45*, 1452.
(49) Alavi, S.; Ripmeester, J. A.; Klug, D. D. *J. Chem. Phys.* **2005**, *123*, 024507.
(50) Inerbaev, T. M.; Belosludov, V. R.; Belosludov, R. V.; Sluiter, M.; Kawazoe, Y. *Comput. Mater. Sci.* **2006**, *36*, 229.
(51) Udachin, K. A.; Lipkowski, J.; Tkacz, M. *Supramol. Chem.* **1994**, *3*, 1981.
(52) Hester, K. C.; Strobel, T. A.; Sloan, E. D.; Koh, C. A. *J. Phys. Chem. B* **2006**, *110*, 14024.
(53) Alavi, S.; Ripmeester, J. A.; Klug, D. D. *J. Chem. Phys.* **2006**, *124*, 014704.
(54) Strobel, T. A.; Taylor, C. J.; Hester, K. C.; Dec, S. F.; Koh, C. A.; Miller, K. T.; Sloan, E. D., Jr. *J. Phys. Chem. B* **2006**, *110*, 17121.
(55) Dyadin, Y. A.; Aladko, E. Y.; Manakov, A. Y.; Zhurko, F. V.; Mikina, T. V.; Komarov, V. Y.; Grachev, E. V. *J. Struct. Chem.* **1999**, *40*, 790.
(56) Uchida, T.; Takeya, S.; Kamata, Y.; Ikeda, I. Y.; Nagao, J.; Ebinuma, T.; Narita, H.; Zatsepina, O.; Buffett, B. A. *J. Phys. Chem. B* **2002**, *106*, 12426.
(57) Mooijer-Van den Heuvel, Ph.D. Thesis. Phase Behavior and Structural Aspects of Ternary Clathrate Hydrate Systems. The Role of Additives, Technische Universiteit Delft, 2004.
(58) Byk, S. S.; Makogon, Y. F.; Fomina, V. I. *Gas hydrates (in Russian*); Chimiya: Moscow, 1980.
(59) Vos, W. L.; Finger, L. W.; Hemley, R. J.; Mao, H. K. *Chem. Phys. Lett.* **1996**, *257*, 524.
(60) Stackelberg, M. V. *Naturwissenschaften* **1949**, *37*, 327.
(61) Alavi, S.; Ripmeester, J. A.; Klug, D. D. *J. Chem. Phys.* **2006**, *125*, 104501.
(62) King, R. B. *Theor. Chim. Acta* **1972**, *25*, 309.
(63) Kosyakov, V. I. *J. Struct. Chem.* **2003**, *44*, 1026.
(64) BES. The storage of hydrogen in semiclathrate material was recently reported at the DOE Annual Program Review (May 16−19, 2006, in Arlington, VA); http://www.hydrogen.energy.gov/pdfs/review06/bes_st11_sloan.pdf.
(65) Shimada, W.; Shiro, M.; Kondo, H.; Takeya, S.; Oyama, H.; Ebinuma, T.; Narita, H. *Acta Crystallogr.* **2005**, *C61*, 65.
(66) Staykova, D. K.; Kuhs, W. F.; Salamatin, A. N.; Hansen, T. *J. Phys. Chem. B* **2003**, *107*, 10299.
(67) Mao, W. L.; Struzhkin, V. V.; Mao, H. K.; Hemley, R. J. *Chem. Phys. Lett.* **2005**, *402*, 66.
(68) Ulivi, L.; Bini, R.; Loubeyre, P.; LeToullec, R.; Jodl, H. J. *Phys. Rev. B* **1999**, *60*, 6502.
(69) Bernasconi, M.; Gaito, S.; Benedek, G. *Phys. Rev. B* **2000**, *61*, 12689.
(70) Spagnolatti, I.; Bernasconi, M.; Benedek, G. *Eur. Phys. J. B* **2003**, *34*, 63.
(71) Menon, M.; Richter, E.; Chernozatonskii, L. *Phys. Rev. B* **2000**, *62*, 15420.
(72) Kasper, J.; Hagenmuller, P.; Pouchard, M.; Cros, C. *Science* **1965**, *150*, 1713.
(73) Yamanaka, S.; Kubo, A.; Inumaru, K.; Komaguchi, K.; Kini, N. S.; Inoue, T.; Irifune, T. *Phys. Rev. Lett.* **2006**, *96*, 076602.
(74) Berg, A. W. C. v. d.; Bromley, S. T.; Flikkema, E.; Wojdel, J.; Maschmeyer, T.; Jansen, J. C. *J. Chem. Phys.* **2004**, *120*, 10285.
(75) Berg, A. W. C. v. d.; Bromley, S. T.; Ramsahye, N.; Maschmeyer, T. *J. Phys. Chem.* **2004**, *108*, 5088.
(76) Ishmaev, S. N.; Sadikov, I. P.; Chernyshov, A. A.; Vindryaevskii, B. A.; Sukhoparov, V. A.; Telepnev, A. S.; Kobelev, G. V. *J. Exp. Theor. Phys.* **1983**, *57*, 228.
(77) Tse, J. S.; Shpakov, V. P.; Belosludov, V. R.; Trouw, F.; Handa, Y. P.; Press, W. *Europhys. Lett.* **2001**, *54*, 354.
(78) Itoh, H.; Chazallon, B.; Schober, H.; Kawamura, K.; Kuhs, W. F. *Can. J. Phys.* **2003**, *81*, 493.
(79) Schober, H.; Tolle, A.; Renker, B.; Heid, R.; Gompf, F. *Phys. Rev. B* **1997**, *56*, 5937.
(80) Iitaka, T.; Ebisuzaki, T. *Phys. Rev. B* **2003**, *68*, 172105.
(81) Militzer, B.; Jenkins, T.; Hemley, R. J.; Struzhkin, V. V.; Mao, H.-K. In preparation.
(82) Tulk, C. A.; Klug, D. D.; Ripmeester, J. A. *J. Phys. Chem. A* **1998**, *102*, 8734.
(83) Goncharov, A. F.; Strzhemechny, M. A.; Mao, H.-k.; Hemley, R. J. *Phys. Rev. B* **2001**, *63*, 064304.
(84) Kranendonk, J. v.; Karl, G. *Rev. Mod. Phys.* **1968**, *40*, 531.
(85) Davidson, D. W.; Ripmeester, J. A. In *Inclusion Compounds*; Atwood, J. L., Davies, J. E. D., MacNichol, D. D., Eds.; Academic Press: London, 1984; Vol. 3.
(86) Ripmeester, J. A.; Ratcliffe, C. I.; Tse, J. S. *J. Chem. Soc., Fraday Trans.* **1988**, *84*, 3731.
(87) Okuchi, T.; Takigawa, M.; Shu, J.; Mao, H.-k.; Hemley, R. J.; Yagi, T. To be published.
(88) Ross, R. G.; Andersson, P.; Backstrom, G. *Nature* **1981**, *290*, 322.
(89) Krivchikov, A. I.; Gorodilov, B. Y.; Korolyuk, O. A.; Manzhelii, V. G.; Romantsova, O. O.; Conrad, H.; Press, W.; Tse, J. S.; Klug, D. D. *Phys. Rev. B* **2006**, *73*, 064203.
(90) Tse, J. S.; White, M. A. *J. Phys. Chem.* **1988**, *92*, 5006.
(91) Gutt, C.; Baumert, J.; Press, W.; Tse, J. S.; Janssen, S. *J. Chem. Phys.* **2002**, *116*, 3795.
(92) Tse, J. S.; Klug, D. D.; Zhao, J. Y.; Sturhahn, W.; Alp, E. E.; Baumert, J.; Gutt, G.; Johnson, M. R.; Press, W. *Nat. Mater.* **2005**, *4*, 917.
(93) Sturhahn, W.; Toellner, T. S.; Alp, E. E.; Zhang, X.; Ando, M.; Seto, M.; Kimball, C. W.; Dabrowski, B. *Phys. Rev. Lett.* **1995**, *74*, 3832.
(94) Andersson, O.; Murashov, V.; White, M. A. *J. Phys. Chem. B* **2002**, *106*, 192.
(95) Handa, Y. P.; Hawkins, R. E.; Murray, J. J. *J. Chem. Thermodyn.* **1984**, *16*, 623.
(96) Handa, Y. P. *J. Phys. Chem.* **1986**, *90*, 5497.
(97) Handa, Y. P. *J. Chem. Thermodyn.* **1986**, *18*, 891.
(98) Handa, Y. P. *J. Chem. Thermodyn.* **1986**, *18*, 915.
(99) Handa, Y. P. *Ind. Eng. Chem. Res.* **1988**, *27*, 872.
(100) White, M. A.; MacLean, M. T. *J. Phys. Chem.* **1985**, *89*, 1380.
(101) Tombari, E.; Presto, S.; Salvetti, G. *J. Chem. Phys.* **2006**, *124*, 154507.
(102) Itoh, H.; Tse, J. S.; Kawamura, K. *J. Chem. Phys.* **2001**, *115*, 9414.
(103) Pauling, L.; Marsh, R. E. *Proc. Natl. Acad. Sci.* **1952**, *38*, 112.
(104) Lunine, J. I.; Stevenson, D. J. *Astrophys. J., Suppl.* **1985**, *58*, 493.
(105) Dyadin, Y. A.; Belosludov, V. R. In *Comprehensive Supramolecular Chemistry*; Elsevier Science Ltd.: Oxford, New York, Tokyo, 1996; Vol. 6.
(106) Belosludov, V. R.; Subbotin, O. S.; Krupskii, D. S.; Prokuda, O. V.; Belosludov, R. V.; Kawazoe, Y. *J. Phys.: Conf. Ser.* **2006**, *29*, 1−7.
(107) Tanaka, H.; Kiyohara, K. *J. Chem. Phys.* **1993**, *98*, 4098.
(108) Tanaka, H.; Kiyohara, K. *J. Chem. Phys.* **1993**, *98*, 8110.
(109) Tanaka, H. *J. Chem. Phys.* **1993**, *101*, 10833.
(110) Tanaka, H. *Can. J. Phys.* **2003**, *81*, 55.
(111) Tanaka, H.; Nakatsuka, T.; Koga, K. *J. Chem. Phys.* **2004**, *121*, 5488.
(112) Tanaka, H. *J. Mol. Liq.* **1995**, *65/66*, 285.
(113) Rodger, P. M. *J. Phys. Chem.* **1990**, *94*, 6080.
(114) Tse, J. S.; Klein, M. L.; McDonald, I. R. *J. Phys. Chem.* **1983**, *87*, 4198.
(115) Klaveren, E. P. v.; Michels, J. P. J.; Schouten, J. A.; Klug, D. D.; Tse, J. S. *J. Chem. Phys.* **2001**, *114*, 5745.
(116) Alavi, S.; Ripmeester, J. A.; Klug, D. D. *J. Chem. Phys.* **2006**, *124*, 204707.
(117) Tse, J. S.; Shpakov, V. P.; Murasov, V. V.; Belosludov, V. R. *J. Chem. Phys.* **1997**, *107*, 9271.
(118) Tse, J. S. *J. Inclusion Phenom.* **1994**, *17*, 259.
(119) Cahill, D. G.; Pohl, R. O. *Annu. Rev. Phys. Chem.* **1988**, *39*, 93.
(120) Ladd, A. J.; Moran, B.; Hoover, W. G. *Phys. Rev. B* **1986**, *34*, 5058.
(121) Iitaka, T.; Ebisuzaki, T. *J. Phys.: Condens. Matter* **2004**, *16*, S1171.
(122) Velde, G. t.; Bickelhaupt, F. M.; Baerends, E. J.; Guerra, C. F.; Gisbergen, S. J. A. v.; Snijders, J. G.; Ziegler, T. *J. Comput. Chem.* **2001**, *22*, 931.
(123) Sluiter, M. H. F.; Belosludov, R. V.; Jain, A.; Belosludov, V. R.; Adachi, H.; Kawazoe, Y.; Higuchi, K.; Otani, T. *Lect. Notes Comput. Sci.* **2003**, *2858*, 330.
(124) Patchkovskii, S.; Yurchenko, S. N. *Phys. Chem. Chem. Phys.* **2004**, *6*, 4152.
(125) Sebastianelli, F.; Xu, M.; Elmatad, Y. S.; Moskowitz, J. W.; Bačić, Z. *J. Phys. Chem. C* **2007**, *111*, 2497.
(126) Xu, M.; Elmatad, Y. S.; Sebastianelli, F.; Moskowitz, J. W.; Bačić, Z. *J. Phys. Chem. B* **2006**, *110*, 24806.
(127) Kumagai, N.; Kawamura, K.; Yokokawa, T. *Mol. Simul.* **1994**, *12*, 177.
(128) Barkalov, O. I.; Klyamkin, S. N.; Efimchenko, V. S.; Antonov, V. E. *JETP Lett.* **2005**, *82*, 413.
(129) McMullan, R. K.; Jeffrey, G. A. *J. Chem. Phys.* **1965**, *42*, 2725.
(130) Mak, T. C. W.; McMullan, R. K. *J. Chem. Phys.* **1965**, *42*, 2732.
(131) Okano, Y.; Yasuoka, K. *J. Chem. Phys.* **2006**, *124*, 024510.
(132) Mao, H. K.; Xu, J.; Bell, P. M. *J. Geophys. Res.* **1986**, *91*, 4673.
(133) Copley, J. R. D.; Neumann, D. A.; Kamitakahara, W. A. *Can. J. Phys.* **1995**, *73*, 763.
(134) Jenkins, T.; Struzhkin, V. V.; Leão, J.; Mao, H.-K., and Hemley, R. J. Submitted.

CR050183D